

HIV gp120 in Lungs of ART-Treated Individuals Impairs Alveolar Macrophage Responses To Pneumococci

Paul J. Collini^{1,6*}, Martin A. Bewley¹, Mohamed Mohasin¹, Helen M. Marriott¹, Robert F. Miller², Anna-Maria Geretti³, Apostolos Beloukas³, Athanasios Papadimitropoulos³, Robert C. Read⁴, Mahdad Noursadeghi⁵, David H. Dockrell^{1,6,7}

1 The Florey Institute for Host-Pathogen Interactions and Department of Infection, Immunity & Cardiovascular Disease, University of Sheffield Medical School, Sheffield, UK

2 Research Department of Infection and Population Health, Institute of Epidemiology & Health Care, Faculty of Population Health Sciences, University College London, London, UK

3. Department of Clinical Infection, Microbiology and Immunology (CIMI), Institute of Infection and Global Health (IGH), University of Liverpool, Liverpool, UK

4. Academic Unit of Clinical and Experimental Sciences, University of Southampton and NIHR Southampton Biomedical Research Centre, Southampton, UK

5. Division of Infection & Immunity, Faculty of Medical Sciences, University College London, London, UK

6. Academic Directorate of Communicable Diseases and Specialised Medicine, Sheffield Teaching Hospitals NHS Foundation Trust, Sheffield, UK

7. MRC/UoE Centre for Inflammation Research, The University of Edinburgh, Edinburgh, UK

***Corresponding Author:** Paul Collini, Department of Infection, Immunity and Cardiovascular Disease, The University of Sheffield Medical School, Beech Hill Rd,

Sheffield, S10 2RX, UK Phone: +44 (0) 114 215 9522 Fax: +44 (0) 114 271 1863 Email: p.collini@sheffield.ac.uk ORCID identifier: 0000-0001-6696-6826

Author contributions

PC and DD conceived this work. Experiments were designed/performed by PC, MB, MM, RR and HM. NM and RM provided technical assistance with HIV-1 infection of macrophages. AM, AB and AP designed and performed ultrasensitive HIV-1 RNA measurement. All authors contributed to preparation and review of the manuscript.

Sources of Support

This is a summary of independent research funded by a Medical Research Council Clinical Training Fellowship (G0901963) to PC and carried out at the National Institute for Health Research (NIHR) Sheffield Clinical Research Facility. MN is supported by NIHR Biomedical Research Centre funding to UCL/UCLH. DHD is supported by MRC grants through COPD-MAP and the SHIELD consortium (MRNO2995X/1). The views expressed are those of the authors and not necessarily those of the MRC, NHS, the NIHR or the Department of Health. HIV-1_{BaL} was obtained through the NIH AIDS Reagent Program Division of AIDS, NIAID, NIH: HIV-1_{Ba-L} from Dr. Suzanne Gartner, Dr. Mikulas Popovic and Dr. Robert Gallo. Recombinant HIV-1LAI/IIIB envelope glycoprotein gp120 (code EVA607) was obtained through the Programme EVA Centre for AIDS Reagents, NIBSC, HPA, Hertfordshire, UK from ImmunoDiagnostics Inc. MA, USA. World Health Organization 3rd International HIV-1 RNA Standard was also obtained from the NIBSC (code:10/152). 14E, 17B and EH21 anti-gp120 human monoclonal antibodies were kindly provided by James E Robinson, Tulane University, New Orleans.

Running Title: gp120 impairs pneumococcal response in HIV lung

Descriptor Number: 10.02 AIDS-Related Lung Disease**Words****Abstract 241****Manuscript, 3551****introduction 306****methods 499****results 1161****discussion 1582****references 47****figures 6 , tables 1,****At a glance summary:****Scientific Knowledge on the Subject:**

Why people living with HIV who are on treatment remain at much greater risk of pneumococcal disease remains unclear.

What This Study Adds to the Field:

This study finds that, despite antiretroviral therapy there is persistent low-level viral replication in the lung. Alveolar macrophages from people living with HIV-1 demonstrate a defect in pneumococcal killing, which is caused by the HIV-1 glycoprotein gp120. This results in reduced susceptibility to macrophage apoptosis, a necessary component for bacterial killing.

This article has an online data supplement, which contains supplemental figures (E1-3) and a detailed description of all materials and methods and is accessible from this issue's table of content online at www.atsjournals.org

Structured Abstract

Rationale

People living with HIV (PLWH) are at significantly increased risk of invasive pneumococcal disease, despite long-term antiretroviral therapy (ART). The mechanism explaining this observation remains undefined.

Objectives

We hypothesized apoptosis-associated microbicidal mechanisms, required to clear intracellular pneumococci that survive initial phagolysosomal killing, are perturbed.

Methods

Alveolar macrophages (AM) were obtained by bronchoalveolar lavage (BAL) from healthy donors or HIV-1-seropositive donors on long-term ART with undetectable plasma viral load. Monocyte-derived macrophages (MDM) were obtained from healthy donors and infected with HIV-1_{BaL} or treated with gp120. Macrophages were challenged with opsonized serotype 2 *Streptococcus pneumoniae* and assessed for apoptosis, bactericidal activity, protein expression and mitochondrial reactive oxygen species (mROS). AM phenotyping, ultra-sensitive HIV-1 RNA quantification and gp120 measurement were also performed in BAL.

Measurements and Main Results

HIV-1_{BaL} infection impaired apoptosis, induction of mROS and pneumococcal killing by MDM. Apoptosis-associated pneumococcal killing was also reduced in AM from ART treated HIV-1-seropositive donors. BAL fluid from these individuals demonstrated persistent lung CD8⁺ T-cell lymphocytosis, and gp120 or HIV-1 RNA was also detected. Despite this, transcriptional activity in AM

freshly isolated from PLWH was broadly similar to healthy volunteers. Instead, gp120 phenocopied the defect in pneumococcal killing in healthy MDM through post-translational modification of Mcl-1, preventing apoptosis induction, caspase activation and increased mROS generation. Moreover gp120 also inhibited mROS dependent pneumococcal killing in MDM.

Conclusions.

Despite ART, HIV-1, via gp120, drives persisting innate immune defects in AM microbicidal mechanisms, enhancing susceptibility to pneumococcal disease.

Abstract Word Count 241

Introduction

HIV-1-seropositive individuals have a significantly increased risk of pneumococcal disease that persists despite antiretroviral therapy (ART), even after CD4⁺ T-cell reconstitution (1, 2). Alveolar macrophages (AM) are essential for pneumococcal clearance from the lung (3) yet evidence of modulation of AM immune competence against pneumococci by HIV-1 has proven elusive; opsonic phagocytosis of pneumococci is preserved during HIV-1 infection (4) and while defective phagolysosomal killing is reported for some pathogens it has not been demonstrated for pneumococci (5).

The capacity of healthy human tissue macrophages to destroy extracellular bacteria through internalization and phagolysosomal killing is finite (6) and AM need to engage a second, delayed microbicidal strategy involving apoptosis-associated killing to eliminate residual viable intracellular pneumococci, which involves combinations of reactive oxygen species (ROS) and nitric oxide (NO) (3, 7-9). The apoptotic program is regulated by the anti-apoptotic Bcl-2 protein Mcl-

1 and induction of a mitochondrial apoptosis pathway (10). Apoptosis-associated killing enhances clearance of pneumococci, limits tissue invasion and downregulates the inflammatory response in the lung (10, 11). Importantly, HIV-1 is associated with an anti-apoptotic gene expression profile in monocytes *in vivo* and promotes macrophage resistance to apoptosis, which contributes to these cells constituting a viral reservoir for HIV-1 (12-15).

We addressed whether HIV-1 prevents engagement of the apoptotic program required for pneumococcal killing. Here we report a selective deficit in delayed, apoptosis-associated pneumococcal killing in AM from ART-treated HIV-1-seropositive volunteers. We document evidence of low level viral replication and gp120 detection in the lung despite long-term suppressive ART and confirm that HIV-1 envelope glycoprotein gp120 is sufficient to inhibit macrophage killing of pneumococci in human monocyte-derived macrophage (MDM), through altered post-translational regulation of Mcl-1 and failure to induce mitochondrial ROS (mROS) generation.

Some of the results of these studies have been previously reported in the form of an abstract and doctoral thesis (16, 17).

Materials and Methods

Additional detail on the method for making these measurements is provided in an online data supplement.

Bacteria, Virus and Infections

Opsonized, type 2 *S. pneumoniae* (D39 strain, NCTC7466) were used for infection of macrophages at a multiplicity of infection of 10 unless otherwise stated, as described (10). In some infections autologous peripheral blood lymphocytes (PBL), or HIV-1_{LAI/IIIIB} envelope glycoprotein gp120 (NIBSC, UK) at 10-100 ng/mL

were added to MDM. HIV-1_{BaL} (NIH AIDS Reagent Program,) was propagated in PBL, then MDM and purified before cell inoculation. Infection rates were measured by intracellular p24 staining as described (18).

Volunteers

Healthy, never smoker, hepatitis B and C virus negative, HIV-1-seropositive patients either established on ART or ART naïve (used as comparator for BAL and virology studies), were recruited from the HIV clinic of STH for bronchoscopy along with matched HIV-seronegative volunteers, described in Table 1.

Cell isolation and culture

Peripheral blood mononuclear cells (PBMC) were isolated from whole blood of healthy donors and differentiated to MDM(10). Non-adherent PBMC were enriched for CD8⁺ T-lymphocytes by negative selection and >95% purity confirmed by flowcytometry. CD8⁺ T-lymphocytes were added 1:1 to MDM. Cells were isolated from bronchoalveolar lavage (BAL) fluid as described (4).

Western blot

Whole cell extracts were isolated using SDS-lysis buffer and separated by SDS gel electrophoresis.

Flow Cytometry

Cell surface marker expression was measured by flow cytometry with fluorophore conjugated antibodies or isotype controls. MDM mROS was measured using MitoSOX-Red (Invitrogen), and loss of $\Delta\psi_m$ with JC-1 (Molecular probes).

Microscopy

Nuclear fragmentation and condensation indicative of apoptosis were detected using 4'6'-diamidino-2-phenylindole (DAPI)(10). BAL cells were identified on stained cytopins.

Caspase activation

Cellular caspase activity was measured using Caspase-Glo 3/7 (Promega) according to the manufacturer's instructions. Luminescence was measured on a Varioskan Flash microplate analyzer (Thermo Scientific).

Quantification of gp120

BAL supernatants were concentrated using 50k Amicon Ultra-filters (Merck Millipore) and gp120 quantified with human monoclonal anti-gp120 antibodies (14E, 17B and EH21), using recombinant gp120 (HIV-1_{LAI/III}) for standards, by ELISA, as described (19).

Metabolic measurements

Oxygen consumption rate (OCR) and extracellular acidification rate (ECAR) were measured using the XF24 extracellular flux analyser (Seahorse, Bioscience) as described (20).

RT-PCR Array

AM gene expression was measured after 48 h with a custom made RT² Profiler PCR Array (SABiosciences) using QPCR.

Ultra-sensitive detection of HIV-1 RNA in BAL

BAL HIV-1 RNA was quantified using a modified version of the Abbott Real-Time HIV-1 assay (Maidenhead, UK), following ultracentrifugation similarly to methods in plasma samples (21). After confirming no inhibition, sensitivity was determined at 1-2 copies per mL by spiking acellular HIV-negative BAL with World Health Organization 3rd International HIV-1 RNA Standard (NIBSC, UK).

Statistics

Results are recorded as mean and SEM unless stated. Sample sizes were informed by standard errors obtained from similar assays in prior publications (10, 20). Analysis was performed with tests, as outlined in the figure legends, using Prism 6.0 software (GraphPad Inc.) and significance defined as $p < 0.05$. Decisions on use of parametric or non-parametric tests were informed by the distribution of the data.

Results

HIV-1 inhibits delayed pneumococcal killing by macrophages

To examine whether HIV-1 influences macrophage killing of pneumococci we infected MDM with HIV-1_{BaL}, an M-tropic strain of HIV-1 (18) or sham virus (Figure 1A) and then, after adjusting for cell numbers, challenged MDM with pneumococci. The numbers of viable intracellular bacteria in MDM 4 h post bacterial challenge, which are the net result of opsonic phagocytosis and phagolysosomal killing (4), were unaltered by HIV-1_{BaL} (Figure 1B). By contrast, 20 h after pneumococcal challenge the intracellular bacterial load was higher in HIV-1_{BaL} MDM (Figure 1C). When we examined engagement of the MDM apoptotic programme we found caspase 3/7 activation, development of apoptotic nuclei and loss of cell numbers following pneumococcal challenge were significantly reduced by HIV-1_{BaL} compared to sham infection (Figure 1D-F). Mcl-1 was down-regulated in sham virus exposed MDM but levels were preserved in HIV-1_{BaL} MDM (Figure 1G-H). Despite comparable mitochondrial density HIV-1_{BaL} MDM had elevated production of mROS after mock-infection

but, unlike sham virus exposed MDM, failed to upregulate mROS after pneumococcal challenge (Figure 1I-J). Overall these findings support a specific deficit in the delayed apoptosis-associated phase of pneumococcal killing in HIV-1_{BaL} MDM.

Impaired apoptosis-associated pneumococcal killing in alveolar macrophages from HIV-1-seropositive individuals treated with ART.

We next investigated whether alveolar macrophages (AM) from the unique lung environment of asymptomatic HIV-1-seropositive individuals established on ART with undetectable plasma HIV-1 viral RNA (Table 1), would also demonstrate impaired pneumococcal clearance. In line with HIV-1_{BaL} infected MDM, AM from ART treated HIV-1-seropositive donors showed a selective defect in delayed pneumococcal killing at 20 h (Figure 2A-B). AM in these samples also showed reductions in caspase 3/7 activation, numbers of apoptotic nuclei and cell loss relative to healthy controls (Figure 2C -E). The impairment of apoptosis following pneumococcal challenge was not related to use of protease inhibitors or non-nucleoside reverse transcriptase inhibitors as the third ART agent (Figure 2F). When we investigated the relationship between the number of HIV-1_{BaL} infected MDM and apoptosis induction following pneumococcal challenge we found no correlation (Figure 2G).

Activation status of AM from HIV-1-seropositive individuals treated with ART is similar to healthy volunteers.

We next investigated if steady state expression of representative genes associated with apoptosis and polarization was altered in AM from our donor groups. Using quantitative PCR arrays we found that while there was an overall trend towards downregulation of gene expression in AM from ART treated HIV-1-seropositive individuals compared with healthy controls, no consistent differences in the expression of these genes was observed (supplemental Figure E1). Furthermore, representative markers of macrophage polarization states CD80 (M1), CD163, CD206 and CD200r (M2) also showed no significant alteration in surface expression in AM from HIV-1-seropositive individuals on ART (supplemental Figure E2).

Impaired bacterial clearance by alveolar macrophages is associated with markers of viral persistence in the lungs of HIV-1-seropositive individuals on ART.

As pulmonary T-lymphocytes influence macrophage-mediated responses to pneumococci in the airway (22), we next sought evidence of alterations to T-lymphocyte numbers in the airway of the asymptomatic HIV-1-seropositive individuals on ART that might link HIV indirectly to the observed AM phenotype. We first analyzed the BAL cell content and included 3 ART-naïve HIV-1-seropositive individuals. Both ART-naïve individuals and those receiving ART had increased lymphocyte numbers in BAL fluid (Figure 3A). Compared to healthy controls, ART-treated HIV-1-seropositive individuals also had a lower percentage of CD4⁺ T-lymphocytes yet a higher proportion of CD8⁺ T-lymphocytes and lower CD4⁺:CD8⁺ T-lymphocyte ratio (Figure 3B-D, Table 1 and supplemental Figure E2). In addition, we found that the ratio of CD4⁺:CD8⁺ T-

lymphocytes in BAL correlated with the induction of AM apoptosis, following pneumococcal challenge (Figure 3F). We next explored whether T-lymphocyte CD38 expression, a marker of immune activation in HIV-1 that correlates with viral load (23), was increased in the ART-treated HIV-1-seropositive donors. However, CD8⁺ T-lymphocytes showed no difference in CD38 expression (Figure 3E). We also tested whether *in vitro* activated, autologous CD8⁺ T-cells, could alter MDM engagement of apoptosis-associated killing but found no modulation of MDM viability, apoptosis or intracellular bacterial survival (supplemental Figure E3A-C).

The CD4:CD8 ratio in ART-treated HIV-1-seropositive individuals is inversely related to the size of the HIV-1 reservoir in the peripheral blood (24). Therefore we considered an alternative possibility that BAL CD4:CD8 ratio was a marker of persistent HIV-1 replication in the lung; we detected HIV-1 p24 in AM cultures from 2/2 ART-naïve and 3/10 ART-treated HIV-1-seropositive donors respectively (Figure 3G). Using ultrasensitive assays HIV-1 RNA was detected at 79 copies/mL and 1-4 copies/mL of cell free BAL fluid supernatants from 1/1 ART-naïve and 2/13 (15.4%) ART-treated HIV-1-seropositive donors respectively. However, the number of donors with detectable p24 or RNA were too few to determine any correlation between these markers of HIV replication and the BAL CD4:CD8 ratio.

gp120 impairs bacterial killing by reducing macrophage susceptibility to apoptosis following pneumococcal challenge

We detected HIV-1 envelope glycoprotein (gp120) in a 10–100ng/mL range in BAL fluid from five of 11 (45.5%) of the ART-treated and in one of two ART-

naïve HIV-1-seropositive donors tested, and observed that those on ART with detectable gp120 also had significantly lower peripheral blood CD4⁺ counts (Figure 4A). Recombinant gp120 recapitulated the selective deficit in delayed phase pneumococcal killing by MDM (Figure 4B-C) and reduced both numbers of apoptotic nuclei and caspase 3/7 activation following pneumococcal challenge (Figure 4D-E). gp120 was also associated with a baseline increase in mROS, without altering mitochondrial density, but gp120 exposed MDM failed to upregulate mROS after pneumococcal challenge (Figure 4F-G). mROS production was abrogated by MitoTEMPO, a mitochondria-targeted superoxide dismutase mimetic that possesses superoxide and alkyl radical scavenging properties, confirming mitochondria as the source of ROS (Figure 4F).

When we analyzed the bioenergetic response of MDM we observed that pneumococcal challenge led to an increase in baseline extracellular acidification rate (ECAR) and a reduction in maximal oxygen consumption rate (OCR Max), and this switch in metabolism was unaltered by gp120 (Figure 4I-L).

Pneumococcal challenge resulted in increased proton leak across the inner mitochondrial membrane (Figure 4M). However, this response and the loss of mitochondrial inner transmembrane potential ($\Delta\psi_m$) were diminished by gp120 (Figure 4H).

We next analysed whether abrogation of mROS upregulation, with an mROS inhibitor MitoTEMPO, altered intracellular pneumococcal killing. After challenging MDM with pneumococci we observed no difference in the number of viable intracellular bacteria after 4 h in the presence of gp120 or mitoTEMPO. However, addition of MitoTEMPO to control MDM increased bacterial survival at

20 h to the same level seen with gp120, but had no effect on viability in gp120 exposed MDM at two distinct multiplicities of infection (Figure 5).

gp120 impairs macrophage apoptosis by altering the post-translational modification of Mcl-1

gp120 prevented downregulation of Mcl-1 (Figure 6A-B) and reduced ubiquitination of Mcl-1 after pneumococcal challenge (Figure 6C-D).

Ubiquitination of Mcl-1 is tightly regulated and ubiquitination is reversed by the de-ubiquitinase (DUB) USP9X (25). We detected decreased expression of USP9X following pneumococcal challenge in control MDM but treatment with gp120 abrogated this response (Figure 6E-F).

Discussion

Here we demonstrate for the first time that HIV-1 impairs pneumococcal killing by macrophages. We show HIV-1 is associated with specific defects in the late phase of pneumococcal killing by impairing apoptosis induction and reducing caspase-dependent induction of mROS. Critically, we find this defect in AM from HIV-1-seropositive individuals established on long-term antiretroviral therapy with good immune reconstitution. Furthermore, despite extended periods of ART we find evidence of altered cellular immune responses, viral replication and release of the HIV-1 envelope glycoprotein gp120 in the lungs. gp120 is sufficient to reprise the deficit in pneumococcal killing and does so via altered post-translational regulation of Mcl-1, a key regulator of macrophage apoptosis.

AM are essential for pneumococcal clearance; they initially resist pro-apoptotic stimuli while engaging phagolysosomal bacterial killing but subsequently activate apoptosis, which facilitates bacterial clearance whilst minimizing inflammation (3, 10). We found that HIV-1_{BaL} impaired host-mediated MDM apoptosis during pneumococcal infection and this was associated with a failure to clear internalized pneumococci. Mcl-1 levels were maintained in the HIV-1_{BaL} infected MDM following pneumococcal challenge while caspase 3/7 activation was reduced, indicating that the mitochondrial pathway of apoptosis, implicated in bacterial killing, was impaired (3, 10). This extends prior observations implicating HIV-1 in altered regulation of Bcl-2 family proteins (13, 26).

Caspase 3 activation promotes release of mROS by inhibiting the mitochondrial electron transport complex I and has been identified as a requirement for the increment of mROS generation that is required to mediate apoptosis-associated killing of intracellular pneumococci (20, 27). The failure of HIV-1_{BaL} infected MDM to increase mROS production over baseline following pneumococcal challenge resulted in pneumococcal survival, similar to recent observations in AM from COPD patients (20). In contrast to the requirement for a late increment in mROS to achieve optimal intracellular killing, chronic baseline elevation of mROS, following HIV-1 or gp120 exposure, does not seem to enhance intracellular bacterial killing. Consistent with this an inhibitor of mROS had no impact on early intracellular bacterial viability at 4 h. COPD AM also show chronic baseline elevation of intracellular mROS but no enhancement of early intracellular bacterial killing (20). To play a role in intracellular killing mROS needs to be generated in proximity to bacteria in phagolysosomes (20, 28) and

be produced at levels above baseline following caspase 3 activation to overwhelm anti-oxidant systems (20). In COPD there is not only reduced caspase 3/7 activation but also an altered balance between mROS generation and superoxide dismutase (SOD) 2 expression, which suggests increased ability to neutralize baseline mROS. Recent observations show gp120 also upregulates SOD in microglia (29). It is noteworthy that, like COPD, HIV-1 has been associated with chronic increases in oxidative stress in mononuclear phagocytes, despite antiretroviral therapy (30, 31), and adaptations to this in both conditions are predicted to impair the capacity to generate a microbicidal response.

HIV-1 infects and replicates in macrophages and, while establishing a long-lived cellular viral reservoir (15), induces resistance to apoptosis (12, 26). Our finding that HIV-1 infection is linked to intrinsic impairments in macrophage apoptotic responses is supported by previous studies with *Mycobacterium tuberculosis* (32), but to the best of our knowledge ours is the first report of impaired killing of pneumococci or any other acute extracellular bacterial infection. Crucially, we have confirmed our findings in clinically relevant AM from aviraemic HIV-1-seropositive individuals.

Untreated, HIV leads to AIDS and increased rates of opportunistic infection, including bacterial pneumonia and IPD (33). Although ART inhibits viral replication, reconstitutes cell mediated immunity and dramatically reduces opportunistic infection, IPD remains 35 fold and bacterial pneumonia 20 fold more common in HIV-1-seropositive individuals in the era of ART (2, 34-36). Our findings suggest that persisting defects in the macrophage microbicidal response contribute to this risk of pneumococcal disease.

We hypothesized that the observed reductions in delayed bacterial killing were due to indirect effects of HIV-1; only a minority of AM in ART-naïve individuals are infected with HIV-1 (37) and, furthermore, within 24 weeks of ART initiation there are large reductions in both BAL fluid RNA and cell-associated HIV-1 nucleic acid (38). Our volunteers had received a median of 75 months ART and had no HIV-1 RNA detectable in peripheral blood by standard assays. Our *in vitro* MDM model allows manipulation of the percentage of MDM that are positive in a culture (18) and we saw no association between the rate of direct MDM HIV-1 infection and apoptosis. Macrophage effector functions are influenced by their activation status (39) and AM from ART-naïve HIV-1-seropositive individuals show classical (M1) activation (37, 40, 41). However, when we measured the activation status and transcriptome of AM from our virally suppressed HIV-1 donors we found no difference from healthy controls. While the plasticity of macrophages makes it conceivable that differences in activation and gene transcription could be lost during AM isolation and culture (40, 42), we conclude that once established on long-term ART, HIV-1 seropositive have no persisting changes in transcriptional pathways regulating AM activation.

T-lymphocytes influence early macrophage-mediated innate immune responses to pneumococci in the airway (22). Consistent with prior reports (38) ART-naïve individuals had increased lymphocyte numbers in BAL fluid but, surprisingly, we also observed persistent lymphocytosis in the BAL of individuals receiving ART. Furthermore, they had a lower CD4:CD8 T-lymphocyte ratio that correlated with altered AM apoptosis. This is a noteworthy finding since low CD4:CD8 ratios in

the peripheral blood of ART-treated HIV-1-seropositive individuals are linked to non-AIDS morbidity, immune activation, inflammation and heightened CD8⁺ T cell activation (43). While there may be a role for specific subsets of CD8⁺ T-lymphocytes influencing AM behavior in the lung, we found no elevated CD38 expression on BAL T-lymphocytes and no effect on apoptosis or bacterial killing when we explored the influence of activated CD8⁺ T-lymphocytes on MDM responses to pneumococci *in vitro*. Thus these suggest that global changes in CD8⁺ T-lymphocytes are a biomarker of intermittent low-level viral replication but do not directly mediate the inhibition of macrophage apoptosis-associated bacterial killing.

We also found evidence for ongoing viral replication in the lungs of some ART-treated individuals by either directly detecting viral RNA, p24 in AM or gp120 in BAL samples. These results add to the observation that potentially replication-competent virus persists in lung AM despite long-term ART (44) and extend reports of detectable gp120 in histological lung specimens of virally suppressed individuals (45). This study measured a snapshot of viral RNA and gp120 and was not powered to detect a relationship between these markers of viral replication and the BAL lymphocyte count or CD4:CD8 ratio. However, the persistence of altered BAL CD4: CD8 T-cell ratios are more likely to be a function of cumulative periods of episodic HIV replication in the lung with normalization of this ratio requiring sustained suppression of viral replication, as described in the peripheral blood (24).

We have been able to demonstrate that recombinant gp120 is sufficient to recapitulate the impairment in delayed phase pneumococcal killing related to HIV-1 infection. HIV-1 envelope (gp120) has been shown to be necessary for macrophage resistance to apoptosis acutely after a single cycle of replication with X4- or R5-tropic HIV-1 (13) while gp120 when disassociated from virus, is sufficient to influence macrophage function and apoptosis resistance (14, 46, 47). Importantly, we observed this effect at concentrations of gp120 similar both to those we found in the BAL and commensurate with those described in other anatomical compartments in HIV-1-seropositive individuals (46).

As with HIV_{BAL}, we observed a failure of gp120 treated MDM to down regulate Mcl-1. Mcl-1 is regulated by ubiquitination and proteasomal degradation (9). Consistent with the paucity of transcriptional changes involving apoptosis regulators in AM from ART-treated HIV-1 donors, we found that gp120 altered post-translational modification of Mcl-1 through reduced ubiquitination in association with upregulation of the DUB USP9X. Thus while Mcl-1 transcriptional upregulation is an immediate intrinsic response to HIV-1 infection (13) we propose that in the context of pneumococcal challenge gp120 mediates the anti-apoptotic phenotype on bystander macrophages through reduced ubiquitination, and the resultant loss of proteasomal degradation of Mcl-1 (10).

gp120 treatment also induced basal mROS but prevented further generation of mROS in response to caspase 3/7 activation following pneumococcal challenge. When we interrogated the bioenergetic response of MDM we observed a switch

to glycolytic metabolism following pneumococcal challenge in keeping with a greater reliance on glycolytic metabolism during innate immune responses associated with classical activation in macrophages. We also observed increased proton leak which is predicted to enhance mROS generation since under these conditions complex I is inhibited by caspase activation (27). However, both the uplift in proton leak and loss of mitochondrial inner membrane potential were diminished by gp120. Taken together these results indicate that despite raised baseline levels gp120 reduces caspase-induction of mROS, a critical microbicidal effector (20, 27, 28).

In conclusion, our findings suggest specific defects in the late phase of pneumococcal killing by AM contribute to the sustained increase in susceptibility to pneumococcal disease in PLWH. Furthermore, despite long-term ART, we find evidence of viral replication resulting in release of gp120 in the lungs associated with HIV-1. Through Mcl-1 mediated inhibition of apoptosis, gp120 reduces caspase-dependent induction of mROS and its important microbicidal effects (20). Significantly the inhibition of apoptosis was not part of a global shift in transcriptional networks regulating cell viability but arose in response to impairment of a critical post-translational pathway that regulates macrophage viability. Since the pathway involves ubiquitination of Mcl-1, and is associated with a critical Mcl-1 deubiquitinase USP9X (25), this pathway merits investigation as a potential therapeutic target.

Acknowledgements

We are grateful for the support of Dr P Carling, Dr S Allen and Professor P Shaw of SITraN, University of Sheffield for the use of and technical help with the Seahorse Extracellular Flux Analyser and Dr C Elliot and colleagues from the Pulmonary Vascular Unit, Sheffield Teaching Hospitals for performing bronchoscopy. The authors declare no competing financial interests.

Study Approval

Healthy donors gave written consent before donating blood for PBMC as approved by the South Sheffield Research Ethics Committee (07/Q2305/7).

HIV-1 seropositive and HIV-seronegative volunteers from the HIV clinics or staff of Sheffield Teaching Hospitals (STH) & the University of Sheffield, Sheffield, UK, gave written informed consent for bronchoalveolar lavage as approved by the NRES Committee Yorkshire & The Humber - South Yorkshire (11/YH/0217).

References

1. Gordin FM, Roediger MP, Girard PM, Lundgren JD, Miro JM, Palfreeman A, Rodriguez-Barradas MC, Wolff MJ, Easterbrook PJ, Clezy K, Slater LN. Pneumonia in HIV-infected persons: increased risk with cigarette smoking and treatment interruption. *Am J Respir Crit Care Med* 2008; 178: 630-636.
2. Yin Z, Rice BD, Waight P, Miller E, George R, Brown AE, Smith RD, Slack M, Delpech VC. Invasive pneumococcal disease among HIV-positive individuals, 2000-2009. *AIDS* 2012; 26: 87-94.
3. Dockrell DH, Marriott HM, Prince LR, Ridger VC, Ince PG, Hellewell PG, Whyte MK. Alveolar macrophage apoptosis contributes to pneumococcal clearance in a resolving model of pulmonary infection. *J Immunol* 2003; 171: 5380-5388.
4. Gordon SB, Molyneux ME, Boeree MJ, Kanyanda S, Chaponda M, Squire SB, Read RC. Opsonic phagocytosis of *Streptococcus pneumoniae* by alveolar macrophages is not impaired in human immunodeficiency virus-infected Malawian adults. *J Infect Dis* 2001; 184: 1345-1349.
5. Collini P, Noursadeghi M, Sabroe I, Miller RF, Dockrell DH. Monocyte and macrophage dysfunction as a cause of HIV-1 induced dysfunction of innate immunity. *Curr Mol Med* 2010; 10: 727-740.
6. Jubrail J, Morris P, Bewley MA, Stoneham S, Johnston SA, Foster SJ, Peden AA, Read RC, Marriott HM, Dockrell DH. Inability to sustain intraphagolysosomal killing of *Staphylococcus aureus* predisposes to bacterial persistence in macrophages. *Cell Microbiol* 2015.

7. Marriott HM, Ali F, Read RC, Mitchell TJ, Whyte MK, Dockrell DH. Nitric oxide levels regulate macrophage commitment to apoptosis or necrosis during pneumococcal infection. *FASEB J* 2004; 18: 1126-1128.

8. Bewley MA, Pham TK, Marriott HM, Noirel J, Chu HP, Ow SY, Ryazanov AG, Read RC, Whyte MK, Chain B, Wright PC, Dockrell DH. Proteomic evaluation and validation of cathepsin D regulated proteins in macrophages exposed to *Streptococcus pneumoniae*. *Mol Cell Proteomics* 2011; 10: M111 008193.

9. Bewley MA, Marriott HM, Tulone C, Francis SE, Mitchell TJ, Read RC, Chain B, Kroemer G, Whyte MK, Dockrell DH. A cardinal role for cathepsin d in coordinating the host-mediated apoptosis of macrophages and killing of pneumococci. *PLoS Pathog* 2011; 7: e1001262.

10. Marriott HM, Bingle CD, Read RC, Braley KE, Kroemer G, Hellewell PG, Craig RW, Whyte MK, Dockrell DH. Dynamic changes in Mcl-1 expression regulate macrophage viability or commitment to apoptosis during bacterial clearance. *J Clin Invest* 2005; 115: 359-368.

11. Marriott HM, Hellewell PG, Cross SS, Ince PG, Whyte MK, Dockrell DH. Decreased alveolar macrophage apoptosis is associated with increased pulmonary inflammation in a murine model of pneumococcal pneumonia. *J Immunol* 2006; 177: 6480-6488.

12. Giri MS, Nebozyhn M, Raymond A, Gekonge B, Hancock A, Creer S, Nicols C, Yousef M, Foulkes AS, Mounzer K, Shull J, Silvestri G, Kostman J, Collman RG, Showe L, Montaner LJ. Circulating monocytes in HIV-1-infected viremic subjects

exhibit an antiapoptosis gene signature and virus- and host-mediated apoptosis resistance. *J Immunol* 2009; 182: 4459-4470.

13. Swingler S, Mann AM, Zhou J, Swingler C, Stevenson M. Apoptotic killing of HIV-1-infected macrophages is subverted by the viral envelope glycoprotein. *PLoS Pathog* 2007; 3: 1281-1290.

14. Yuan Z, Fan X, Staitieh B, Bedi C, Spearman P, Guidot DM, Sadikot RT. HIV-related proteins prolong macrophage survival through induction of Triggering receptor expressed on myeloid cells-1. *Sci Rep* 2017; 7: 42028.

15. Lum JJ, Badley AD. Resistance to apoptosis: mechanism for the development of HIV reservoirs. *Curr HIV Res* 2003; 1: 261-274.

16. Collini P. The modulation of macrophage apoptosis by HIV-1 during *Streptococcus pneumoniae* infection. Faculty of Medicine, Dentistry and Health. White Rose eTheses Online: University of Sheffield; 2016.

17. Collini PJ, Bewley M, Greig JM, Bowman C, Dockrell DH. HIV gp120 in the Lungs of HAART Treated Individuals Impairs Pulmonary Immunity Conference on Retroviruses and Opportunistic Infections Boston, Massachusetts; 2016.

18. Tsang J, Chain BM, Miller RF, Webb BL, Barclay W, Towers GJ, Katz DR, Noursadeghi M. HIV-1 infection of macrophages is dependent on evasion of innate immune cellular activation. *AIDS* 2009; 23: 2255-2263.

19. Rychert J, Strick D, Bazner S, Robinson J, Rosenberg E. Detection of HIV gp120 in plasma during early HIV infection is associated with increased

proinflammatory and immunoregulatory cytokines. *AIDS Res Hum Retroviruses* 2010; 26: 1139-1145.

20. Bewley MA, Preston JA, Mohasin M, Marriott HM, Budd RC, Swales J, Collini P, Greaves DR, Craig RW, Brightling CE, Donnelly LE, Barnes PJ, Singh D, Shapiro SD, Whyte MKB, Dockrell DH. Impaired Mitochondrial Microbicidal Responses in Chronic Obstructive Pulmonary Disease Macrophages. *Am J Respir Crit Care Med* 2017; 196: 845-855.

21. Ruggiero A, De Spiegelaere W, Cozzi-Lepri A, Kiselinova M, Pollakis G, Beloukas A, Vandekerckhove L, Strain M, Richman D, Phillips A, Geretti AM, Group ES. During Stably Suppressive Antiretroviral Therapy Integrated HIV-1 DNA Load in Peripheral Blood is Associated with the Frequency of CD8 Cells Expressing HLA-DR/DP/DQ. *EBioMedicine* 2015; 2: 1153-1159.

22. Zhang Z, Clarke TB, Weiser JN. Cellular effectors mediating Th17-dependent clearance of pneumococcal colonization in mice. *J Clin Invest* 2009; 119: 1899-1909.

23. Barry SM, Johnson MA, Janossy G. Increased proportions of activated and proliferating memory CD8+ T lymphocytes in both blood and lung are associated with blood HIV viral load. *J Acquir Immune Defic Syndr* 2003; 34: 351-357.

24. Boulassel MR, Chomont N, Pai NP, Gilmore N, Sekaly RP, Routy JP. CD4 T cell nadir independently predicts the magnitude of the HIV reservoir after prolonged suppressive antiretroviral therapy. *J Clin Virol* 2012; 53: 29-32.

25. Mojsa B, Lassot I, Desagher S. Mcl-1 ubiquitination: unique regulation of an essential survival protein. *Cells* 2014; 3: 418-437.
26. Zhang M, Li X, Pang X, Ding L, Wood O, Clouse KA, Hewlett I, Dayton AI. Bcl-2 upregulation by HIV-1 Tat during infection of primary human macrophages in culture. *J Biomed Sci* 2002; 9: 133-139.
27. Ricci JE, Gottlieb RA, Green DR. Caspase-mediated loss of mitochondrial function and generation of reactive oxygen species during apoptosis. *J Cell Biol* 2003; 160: 65-75.
28. West AP, Brodsky IE, Rahner C, Woo DK, Erdjument-Bromage H, Tempst P, Walsh MC, Choi Y, Shadel GS, Ghosh S. TLR signalling augments macrophage bactericidal activity through mitochondrial ROS. *Nature* 2011; 472: 476-480.
29. Samikkannu T, Ranjith D, Rao KV, Atluri VS, Pimentel E, El-Hage N, Nair MP. HIV-1 gp120 and morphine induced oxidative stress: role in cell cycle regulation. *Front Microbiol* 2015; 6: 614.
30. Elbim C, Pillet S, Prevost MH, Preira A, Girard PM, Rogine N, Hakim J, Israel N, Gougerot-Pocidallo MA. The role of phagocytes in HIV-related oxidative stress. *J Clin Virol* 2001; 20: 99-109.
31. Sharma B. Oxidative stress in HIV patients receiving antiretroviral therapy. *Curr HIV Res* 2014; 12: 13-21.
32. Patel NR, Zhu J, Tachado SD, Zhang J, Wan Z, Saukkonen J, Koziel H. HIV impairs TNF-alpha mediated macrophage apoptotic response to Mycobacterium tuberculosis. *J Immunol* 2007; 179: 6973-6980.

33. Janoff EN, Breiman RF, Daley CL, Hopewell PC. Pneumococcal disease during HIV infection. Epidemiologic, clinical, and immunologic perspectives. *Ann Intern Med* 1992; 117: 314-324.
34. Grau I, Pallares R, Tubau F, Schulze MH, Llopis F, Podzamczar D, Linares J, Gudiol F. Epidemiologic changes in bacteremic pneumococcal disease in patients with human immunodeficiency virus in the era of highly active antiretroviral therapy. *Arch Intern Med* 2005; 165: 1533-1540.
35. Sogaard OS, Lohse N, Gerstoft J, Kronborg G, Ostergaard L, Pedersen C, Pedersen G, Sorensen HT, Obel N. Hospitalization for pneumonia among individuals with and without HIV infection, 1995-2007: a Danish population-based, nationwide cohort study. *Clin Infect Dis* 2008; 47: 1345-1353.
36. Jordano Q, Falco V, Almirante B, Planes AM, del Valle O, Ribera E, Len O, Pigrau C, Pahissa A. Invasive pneumococcal disease in patients infected with HIV: still a threat in the era of highly active antiretroviral therapy. *Clin Infect Dis* 2004; 38: 1623-1628.
37. Jambo KC, Banda DH, Kankwatira AM, Sukumar N, Allain TJ, Heyderman RS, Russell DG, Mwandumba HC. Small alveolar macrophages are infected preferentially by HIV and exhibit impaired phagocytic function. *Mucosal Immunol* 2014.
38. Twigg HL, Weiden M, Valentine F, Schnizlein-Bick CT, Bassett R, Zheng L, Wheat J, Day RB, Rominger H, Collman RG, Fox L, Brizz B, Dragavon J, Coombs RW, Bucy RP. Effect of highly active antiretroviral therapy on viral burden in the lungs of HIV-infected subjects. *J Infect Dis* 2008; 197: 109-116.

39. Xue J, Schmidt SV, Sander J, Draffehn A, Krebs W, Quester I, De Nardo D, Gohel TD, Emde M, Schmidleithner L, Ganesan H, Nino-Castro A, Mallmann MR, Labzin L, Theis H, Kraut M, Beyer M, Latz E, Freeman TC, Ulas T, Schultze JL. Transcriptome-based network analysis reveals a spectrum model of human macrophage activation. *Immunity* 2014; 40: 274-288.
40. Buhl R, Jaffe HA, Holroyd KJ, Borok Z, Roum JH, Mastrangeli A, Wells FB, Kirby M, Saltini C, Crystal RG. Activation of alveolar macrophages in asymptomatic HIV-infected individuals. *J Immunol* 1993; 150: 1019-1028.
41. Gordon SB, Jagoe RT, Jarman ER, North JC, Pridmore A, Musaya J, French N, Zijlstra EE, Molyneux ME, Read RC. The alveolar microenvironment of patients infected with human immunodeficiency virus does not modify alveolar macrophage interactions with *Streptococcus pneumoniae*. *Clin Vaccine Immunol* 2013; 20: 882-891.
42. Tomlinson GS, Booth H, Petit SJ, Potton E, Towers GJ, Miller RF, Chain BM, Noursadeghi M. Adherent human alveolar macrophages exhibit a transient pro-inflammatory profile that confounds responses to innate immune stimulation. *PLoS One* 2012; 7: e40348.
43. Serrano-Villar S, Perez-Elias MJ, Dronda F, Casado JL, Moreno A, Royuela A, Perez-Molina JA, Sainz T, Navas E, Hermida JM, Quereda C, Moreno S. Increased risk of serious non-AIDS-related events in HIV-infected subjects on antiretroviral therapy associated with a low CD4/CD8 ratio. *PLoS One* 2014; 9: e85798.

44. Cribbs SK, Lennox J, Caliendo AM, Brown LA, Guidot DM. Healthy HIV-1-infected individuals on highly active antiretroviral therapy harbor HIV-1 in their alveolar macrophages. *AIDS Res Hum Retroviruses* 2015; 31: 64-70.
45. Gundavarapu S, Mishra NC, Singh SP, Langley RJ, Saeed AI, Feghali-Bostwick CA, McIntosh JM, Hutt J, Hegde R, Buch S, Sopori ML. HIV gp120 induces mucus formation in human bronchial epithelial cells through CXCR4/alpha7-nicotinic acetylcholine receptors. *PLoS One* 2013; 8: e77160.
46. Cummins NW, Rizza SA, Badley AD. How much gp120 is there? *J Infect Dis* 2010; 201: 1273-1274; author reply 1274-1275.
47. Cicala C, Arthos J, Selig SM, Dennis G, Jr., Hosack DA, Van Ryk D, Spangler ML, Steenbeke TD, Khazanie P, Gupta N, Yang J, Daucher M, Lempicki RA, Fauci AS. HIV envelope induces a cascade of cell signals in non-proliferating target cells that favor virus replication. *Proc Natl Acad Sci U S A* 2002; 99: 9380-9385.

Figure legends

Figure 1 HIV-1_{BaL} infection is associated with reduced apoptosis-associated pneumococcal killing by macrophages.

Representative photomicrographs of human monocyte-derived macrophages (MDM) challenged with HIV-1_{BaL} or sham virus and stained for the presence of p24 (blue) (A). Scale bar = 50 μ m. Sham or HIV-1_{BaL} MDM were challenged with *S. pneumoniae* (D39) for 4 h (B) or 20 h (C), and lysed to determine the log colony forming units (CFU)/ml, n=15, *=p<0.05, paired Student's t-test.

Alternatively MDM were challenged with D39 or mock infected (MI) for 16 h and caspase 3/7 luminescence measured (D), n=11, *=p<0.05, paired Student's t-test, or for 20 h and the percentage of apoptotic nuclei (E) or cells per high per field (hpf) estimated (F), both n=14, ***=p<0.001, *=p<0.05, 2 way ANOVA.

Additionally cells were challenged for 20 h then lysed and western blot performed for estimation of Mcl-1 (G) and densitometry performed (H), or challenged for 16 h and stained with Mitotracker to estimate mitochondrial density with relative fluorescence units (RFU) (I) or with MitoSOX to estimate fold induction of mitochondrial reactive oxygen species (mROS) vs. sham infection (J), both n=5, **p<0.01, *=p<0.05, 2 way ANOVA.

Figure 2 People living with HIV have impaired alveolar macrophage apoptosis associated killing of pneumococci

Alveolar macrophages (AM) from ART treated HIV-1⁺ (ART) or control donors were challenged with *S. pneumoniae* (D39) for 4 h (A) n=8/12 or 20 h (B) n=7/12 and numbers of viable intracellular bacteria determined, *=p<0.05,

unpaired Student's t-test. Alternatively HIV-1-seropositive or control AM were exposed to D39 or mock infected (MI) for 16 h and caspase 3/7 activity measured (C), $n=5/11$, $*=p<0.05$, unpaired Student's t-test or for 20 h and nuclear features of apoptosis recorded (D) or cell numbers assessed (E) both $n=8/14$, $**=p<0.01$, $***=p<0.001$, 2 way ANOVA. Nuclear features of apoptosis in AM were determined separately from HIV-1-seropositive donors who had used non-nucleoside reverse transcriptase inhibitor (NNRTI) or protease inhibitor (PI) exclusively as the third ART agent (F), $n=7/6$. HIV-1_{BaL} or sham-virus exposed monocyte-derived macrophages (MDM) were challenged D39 for 20 h and apoptosis assessed by nuclear morphology. The value for the HIV-1_{BaL} apoptosis increment was subtracted from the value for the sham-virus exposed MDM increment to calculate the $\Delta\%$ apoptosis and plotted against the percentage of p24⁺ positive MDM, measured by immunohistochemistry $n=13$ (G).

Figure 3 People living with HIV have altered T-lymphocyte numbers in the lung associated with markers of viral replication

Bronchoalveolar lavage (BAL) cells were isolated from HIV-1-seronegative (control $n=10$) and ART-naïve HIV-1-seropositive (naïve, $n=3$) or ART-treated HIV-1-seropositive (ART $n=14$) donors and the percentage lymphocytes determined from cytopins (A). Flow cytometry was used to estimate the percentages of CD3⁺CD4⁺ and CD3⁺CD8⁺ BAL lymphocytes for controls ($n=6$) and ART-treated ($n=11$) and the mean ratio of CD4⁺:CD8⁺ lymphocytes calculated for each (3.79 ± 0.76 and 1.16 ± 0.15 respectively)(B-D and supplemental figure 2), $**=p<0.01$, Mann Whitney test, or the expression of CD38 on CD3⁺CD8⁺ BAL

lymphocytes (controls n=5, ART n= 9)(E). The ratio correlated to levels of AM apoptosis (n=15)(F), ** p<0.01, Pearson. AM from ART donors were stained with anti-p24 and XGal conjugated secondary antibodies (G). The photomicrograph demonstrates blue p24 positive AM and is representative of photomicrographs from 3 donors, scale bar = 50 μ m.

Figure 4 gp120 modifies mitochondrial ROS production following pneumococcal challenge and impairs bacterial killing

gp120 was measured by sandwich ELISA in the bronchoalveolar lavage (BAL) fluid from 11 ART treated HIV-1 seropositive donors and peripheral blood CD4+ counts were compared in HIV-1-seropositive donors with and without detectable gp120 in the BAL (A), n=5/6, **=p<0.01, Mann Whitney test. Monocyte-derived macrophages (MDM) were treated with 10ng/mL gp120 or media then challenged with *S. pneumoniae* (D39) and viable intracellular bacteria (cfu) were estimated after 4 h (B) and 20 h (C), n=15, *=p<0.05, paired Student's t-test, or nuclear features of apoptosis estimated after 20 h incubation and compared with mock infection (MI)(D), n=8, *=p<0.05, 2 way ANOVA. Alternatively MDM were treated with 100ng/mL gp120 or media then challenged with D39 or mock infected (MI) for 16 h before quantifying caspase 3/7 activity (E), n=7, *=p<0.05, paired Student's t-test, mitochondrial reactive oxygen species (mROS), in the presence or absence of MitoTEMPO (mT) (F), n=4-8, **=p< 0.01 2 way ANOVA, #=p<0.005 Mann Whitney test (vs. no mT), mitochondrial density (G), n=4, loss of mitochondrial inner transmembrane potential ($\Delta\psi_m$), (H), n=3, *=p<0.05, **=p< 0.01, 2 way ANOVA or using a Seahorse XF24 extracellular flux analyzer to measure oxygen consumption rate

(OCR) (I) and extracellular acidification rate (ECAR) (K) and calculate maximum OCR (J), basal ECAR (L) and proton leak (M), all n=6, *=p<0.05, **=p< 0.01, ***=p<0.001, ****=p<0.0001, 2 way ANOVA. Oligo (oligomycin A), Rot (rotenone), AntA (antimycin A).

Figure 5 mROS dependent intracellular pneumococcal killing in macrophages is inhibited by gp120 treatment.

Monocyte-derived macrophages (MDM) were treated with 100ng/mL gp120 or media in the presence of vehicle or MitoTEMPO (mT) then challenged with *S. pneumoniae* (D39) at multiplicity of infection 10 (A) or 100 (B) and viable intracellular bacteria (cfu) were estimated after 4 h and 20 h, n=5 (A), or 20 h n=6 (B) ****=p<0.0001, *=p<0.05 vs 20 h control, 1 way ANOVA.

Figure 6 gp120 modulates post-translational regulation of Mcl-1 in MDM following pneumococcal challenge.

Monocyte-derived macrophages (MDM) were treated with 100ng/mL gp120 or media then challenged with *S. pneumoniae* (D39) or mock infected (MI) before lysing cells at 20 h and performing Western blots to estimate Mcl-1 (A-B) or lysing cells at 16 h and performing ubiquitin pull-down followed by western blotting for Mcl-1 or total ubiquitinated proteins (C-D). Alternatively cells were lysed at 20 h and blotted for USP9X (E-F). In each case a representative western blot is depicted with the result of densitometry performed on three separate western blots with data shown as fold change in band density compared with mock infected control MDM after adjustment for any fold change in loading control, *=p<0.05, **=p<0.01, 2 way ANOVA.

Tables**Table 1 Healthy and HIV-1 seropositive alveolar macrophage donors**

	HIV-1 on ART	HIV-1 ART- NAÏVE	CONTROL
	n or mean \pm SEM		
Age (years)	42.4 \pm 2.4	41.7 \pm 5.3	40.8 \pm 2.7
Sex			
Male	8	3	8
Female	6	0	4
Ethnicity			
White	9	3	9
Black African	4	0	3
other	1	0	0
Nadir CD4 (cells/mm ³)	213 \pm 26	587 \pm 105	n/a
CD4 (cells/mm ³)	643 \pm 51	672 \pm 176	n/a
CD4:CD8	0.83 \pm 0.07	0.66 \pm 0.003	n/a
plasma HIV-1 RNA (log ₁₀ copies/mL)	undetectable	4.43 \pm 3.84	n/a
3 rd ART agent			
PI	6	n/a	n/a
NNRTI	7	n/a	n/a
Mixed / other regimen	1	n/a	n/a
Duration (months)	75 (43-108)*		

* median with interquartile range, PI = Protease Inhibitor, NNRTI = Non-Nucleoside Reverse Transcriptase Inhibitor

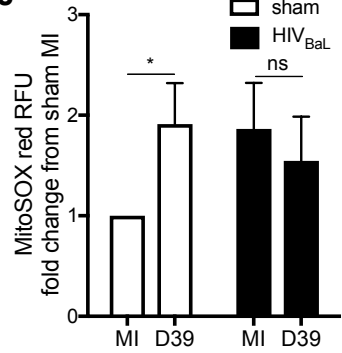
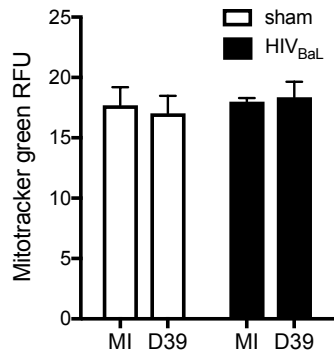
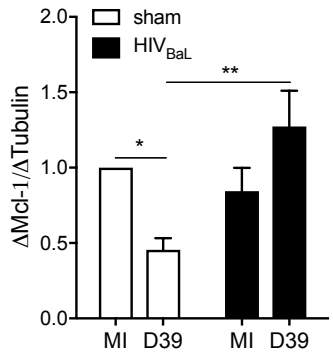
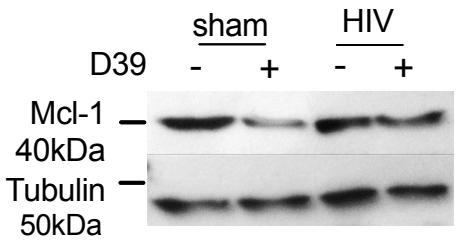
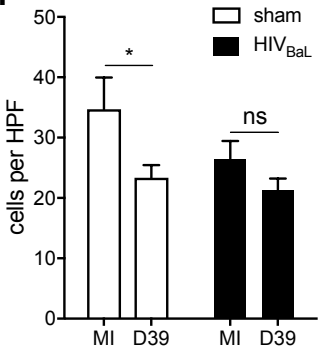
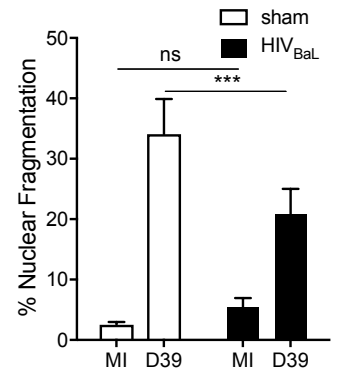
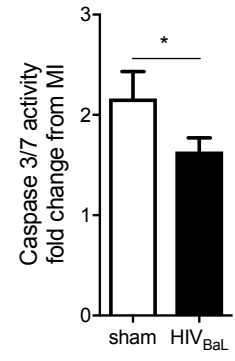
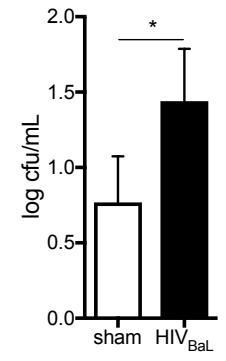
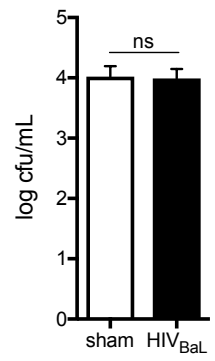
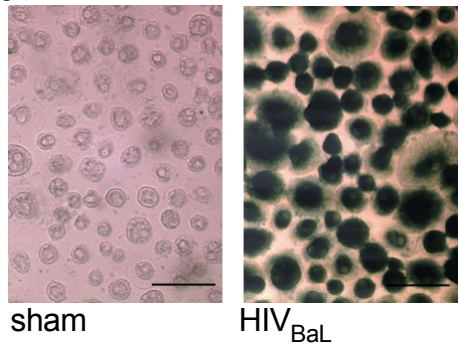


Figure 1

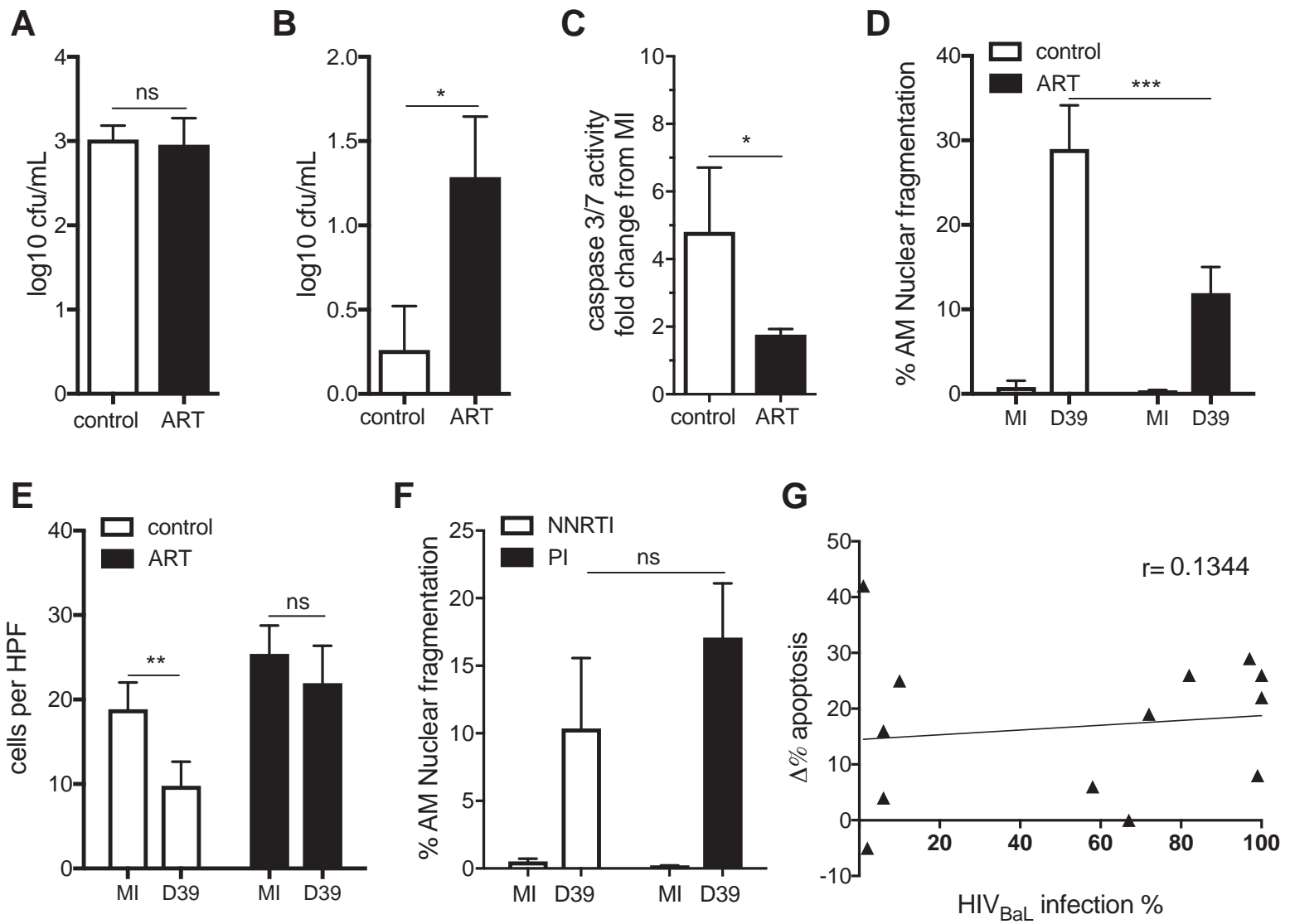


Figure 2

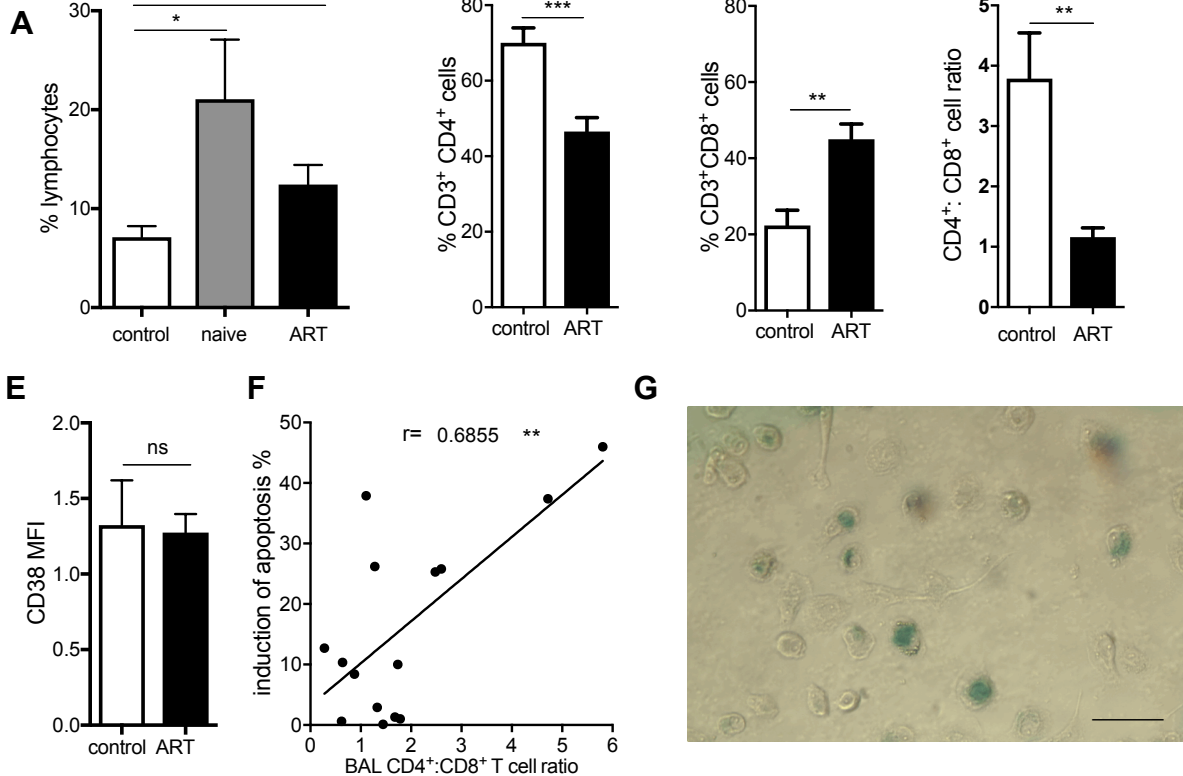


Figure 3

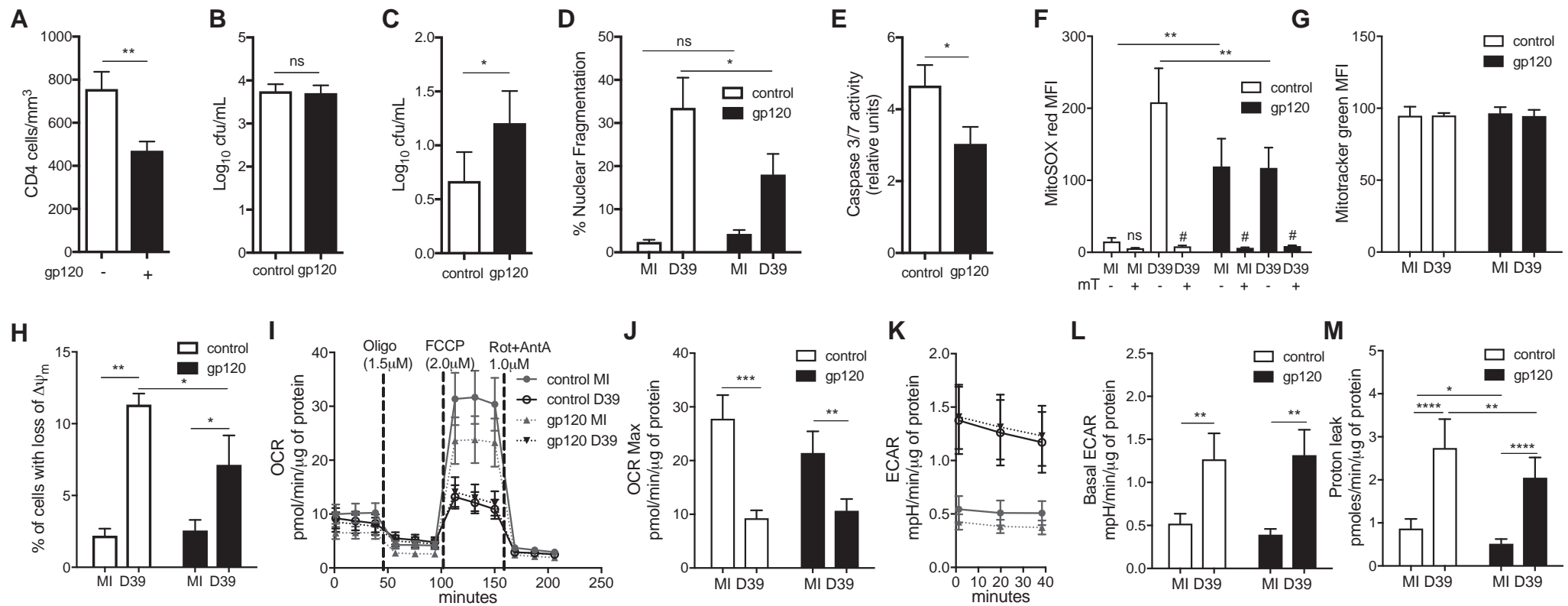


Figure 4

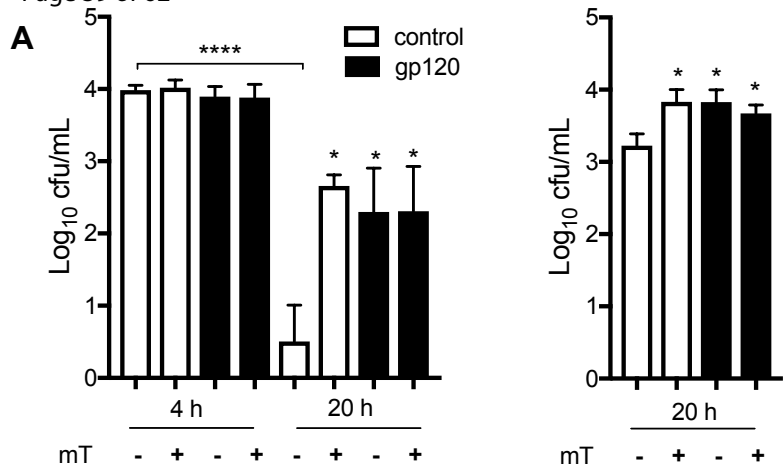


Figure 5

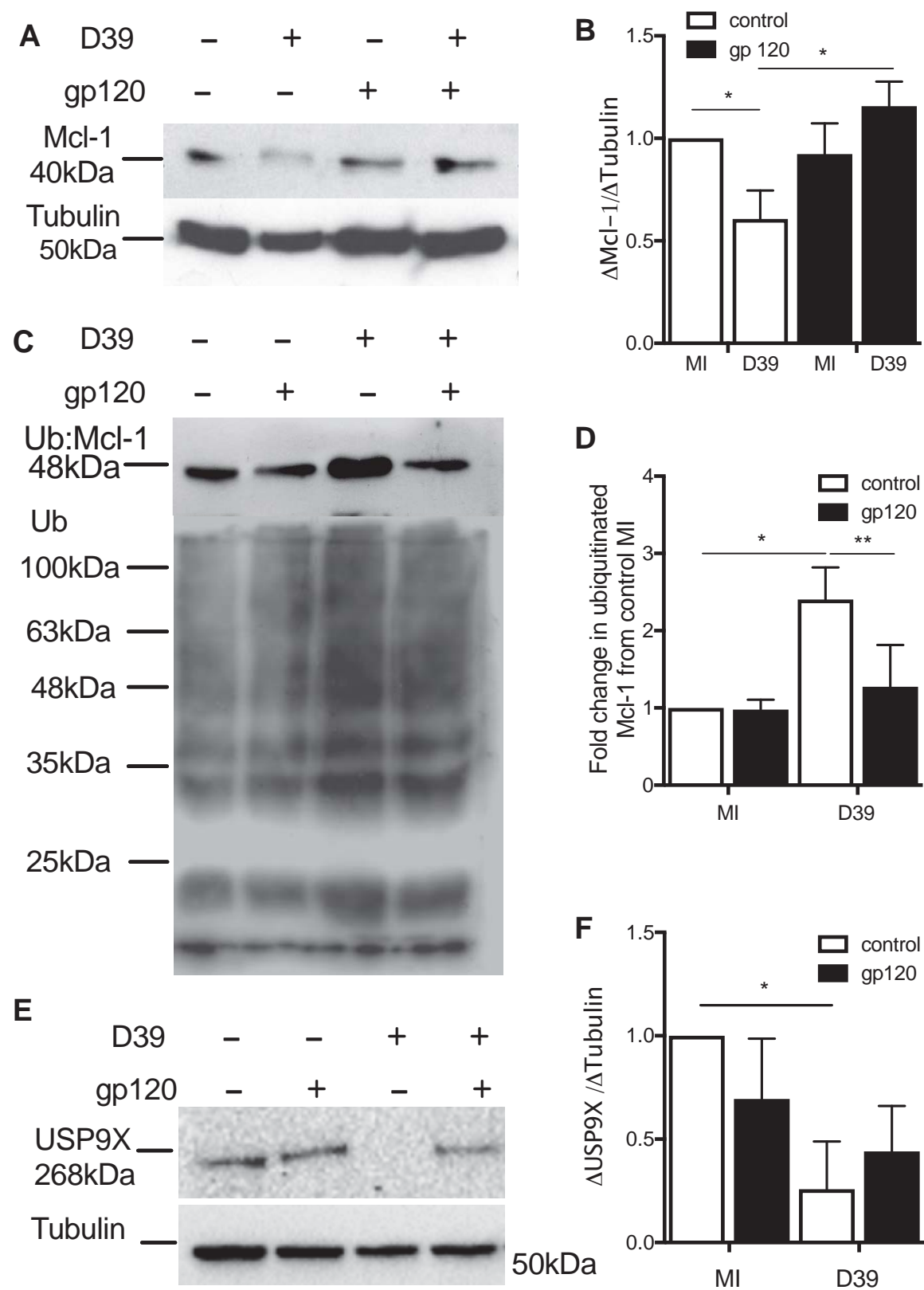


Figure 6

Supplemental Materials and Methods

Volunteers

Alveolar macrophages (AM) and lymphocytes were isolated from bronchoalveolar lavage (BAL) fluid obtained from healthy, never smoker, hepatitis B and C virus negative HIV-1 seropositive and HIV-seronegative volunteers (Table I). HIV-1-seropositive individuals were recruited from the HIV clinics of Sheffield Teaching Hospitals. 14 were established on ART and 13 had used either Non Nucleoside Reverse Transcriptase Inhibitors (NNRTI) (7 donors) or Protease Inhibitors (PI) (6 donors) exclusively as the third agent in their ART regimen. 3 ART naïve patients were also included for evaluation of BAL cell counts, HIV RNA and gp120 measurements only. Whole blood for human peripheral blood mononuclear cell (PBMC) isolation was collected from healthy volunteer donors.

Bacteria Type 2 *S. pneumoniae* (D39 strain, NCTC7466) were grown to mid log phase as previously described (2). D39 were opsonized in RPMI (Sigma-Aldrich) containing 10% anti-pneumococcal immune serum, with detectable levels of antibody, as previously described (2). Opsonized D39 at a multiplicity of infection (MOI) of 10 (unless otherwise stated in the Figure legends) or media alone (mock infection) were added to wells and incubated at 4°C for 1 h (to maximize adherence) and then at 37°C for 3 h (to maximize internalization). Cultures were washed 3 times in PBS to remove non-adherent bacteria, then incubated for a further 12-16 h in RPMI 1640 (Lonza) with 10% decompartmented fetal bovine serum (FBS; Bioclear). In certain experiments, either 10-100 ng/mL recombinant HIV-1_{LAI/IIIIB} envelope glycoprotein gp120 (obtained through the Programme EVA Centre for AIDS Reagents, NIBSC, HPA, UK from ImmunoDiagnostics

Inc. MA, USA) or autologous lymphocytes were added to MDM from 1-2 h prior to infection and after washing at 4 h.

Virus. CCR5 tropic HIV-1_{BaL} (obtained through the NIH AIDS Reagent Program, Division of AIDS, NIAID, NIH: HIV-1_{BaL} from Dr. Suzanne Gartner, Dr. Mikulas Popovic and Dr. Robert Gallo) was propagated for 3-4 d in IL-2 (PeproTech) maintained peripheral blood lymphocytes (PBL) and then 7 d in MDM differentiated in RPMI + 10% autologous human serum with 20 ng/mL macrophage colony-stimulating factor (M-CSF, R&D Systems). Culture supernatants were ultracentrifuged through a 20% sucrose buffer and re-suspended in 10% FBS-RPMI after each passage (3). Replication competent HIV-1 virus preparations were titrated on the NP2 astrocytoma cell line stably transfected with CD4 and CCR5 and stained for intracellular p24 (3).

Isolation and culture of macrophages and other leukocytes. PBMC were isolated by Ficoll-Paque (Pharmacia-Amersham) density centrifugation of whole blood from healthy donors as described previously (2). PBMC were plated at 2×10^6 cells/mL in RPMI 1640 media with 2 mmol/L L-glutamine (Gibco BRL) containing 10% human AB serum (First Link) in 24-well plates (Costar). After 24 h, non-adherent cells were removed and adherent cells were cultured in in 5% CO₂ at 37°C in either 10% FBS-RPMI for 14 days. Prior to use, representative wells were scraped to determine the concentration of MDM prior to challenge with D39 or HIV-1_{BaL}. Peripheral blood lymphocytes (PBL) were purified from PBMC by performing 2 plastic adherence steps to remove monocytes. For HIV-1_{BaL} propagation PBL were re-suspended at 1×10^6 cells/mL in RPMI 1640 +10% AB serum with 20 µg/mL interleukin (IL)-2 (PeproTech) and 0.5 µg/mL phytohemagglutinin (PHA, Sigma-Aldrich). For syngeneic co-culture experiments, PBL were enriched for CD8⁺ T cells by negative selection using the Easy Sep Human CD8⁺ T

cell enrichment Kit (Stem cell technologies) as per the manufacturer's instructions and re-suspended at 1×10^6 cells/mL. Purity of >95% was confirmed by flowcytometry. CD8⁺ T cells were activated over 2 h using Dynabeads Human T-Activator CD3/CD28 (Life technologies) according to the manufacturer's instructions then added 1:1 to MDM cultures from the same donor for D39 challenge.

AM were isolated as previously described (4). Briefly, lavage with ≤ 200 mL of warm sterile saline was carried out after the bronchoscope was lodged in a middle-lobe subsegmental bronchus +/- midazolam sedation by a consultant respiratory physician, and BAL fluid was aspirated under 23kPa suction pressure and collected in a pre-cooled trap (Argyle™, Coviden). BAL fluid volume was documented then sieved through sterile gauze, centrifuged at $400g \times 10$ minutes and supernatant frozen at -80 °C. The pellets were resuspended in RPMI 1640 + 10% AB serum + 40 u/mL penicillin (Lonza) + $40 \mu\text{g mL}^{-1}$ streptomycin (Lonza) + $0.5 \mu\text{g/mL}$ amphotericin (Fungizone™, GIBCO) at a density of 2×10^5 AM/mL. 100 μL was diluted 1:1 with HIFCS and fixed to prepare a cytopsin slide. Suspensions that contained visible red blood cells were subjected to Ficoll-Paque density centrifugation and re-suspended. Cells were incubated overnight at 37°C in 5% CO_2 in 6, 24 and 96 well cell culture plates (Costar). The following day medium with non-adherent cells was replaced with fresh antibiotic free FBS-RPMI. The non-adherent cells from each donor were pooled and prepared for flow analyses. Adherent AM were cultured until use on the third day of incubation.

HIV infection of MDM. 7 day MDM were inoculated with doses of HIV-1_{BaL} equivalent to MOI of 0.1-1.0 or sham virus (prepared from the same, uninoculated, PBL/MDM propagation) for 16 h and then incubated in fresh FBS-RPMI for a further 7 d.

Intracellular p24 staining. NP2, MDM or AM were fixed and permeabilized in an ice-cold mixture 1:1 of pure acetone and methanol, washed and incubated with 1:25 p24 antibody (IgG1k monoclonal antibody to HIV-1 gag p24, code no. E366, obtained through the Programme EVA Centre for AIDS Reagents, NIBSC, UK from Dr B Wahren) then 5 µg/mL goat anti-mouse antibody conjugated to β-galactosidase (Southern Biotechnology Associates), each for 1 h, then overnight at 37 °C in a galactosidase substrate solution of 0.5 mgmL⁻¹ 5-bromo-4-chloro-3-indolyl—galactopyranoside (X-gal, Melford) in PBS containing 3 mmol/L potassium ferricyanide (FLUKA), 3 mmol/L potassium ferrocyanide (FLUKA) and 1 mmol/L magnesium chloride (Sigma). Blue stained cells positive for p24 were counted by microscope to provide a virus titre or number and proportion of infected cells (3).

SDS-PAGE and Western blotting. Whole cell extracts were lysed on ice in buffer containing 20mM TRIS-HCl pH7.4, 5mM ethylenediaminetetraacetic acid (EDTA), mM ethylene glycol tetraacetic acid (EGTA), 150mM NaCl and 1% sodium dodecyl sulphate (SDS), with protease inhibitor cocktail (Complete™, Roche). Protein was quantified using a modified Lowry protocol (DC Protein Assay, Biorad) and protein was loaded equally per lane and separated by 12% SDS-PAGE then blotted onto nitrocellulose membranes (Bio-Rad Laboratories) with protein transfer confirmed by Ponceau S staining. Blots were blocked for 60 min at room temperature in PBS containing 0.05% Tween with 5% (v/w) skim milk powder then incubated overnight with anti-Mcl-1 (rabbit polyclonal, 1:1000 S-19, Santa Cruz, recognizing full length Mcl-1, 40 kDa and ubiquitinated Mcl-1,

>40 kDa) or anti-ubiquitin (Pierce Scientific 1:500) or anti-USP9X (rabbit polyclonal, 1:2500, Bethyl Laboratories) with anti-tubulin (mouse monoclonal, 1:2000, Sigma-Aldrich) or anti-actin (rabbit polyclonal, 1:5000 Sigma-Aldrich) as loading controls. Proteins were detected using HRP-conjugated secondary antibodies (1:2000; Dako) and enhanced chemiluminescence (ECL) (Amersham Pharmacia). The density of bands was measured using ImageJ™ software v1.440 (NIH). Fold change from mock-infected was calculated and normalized to the fold change in loading control (2, 5).

Ubiquitin pull-down assay. Cells were lysed in M-PER Mammalian Protein Extraction Reagent (Thermo Scientific) and ubiquitinated proteins were isolated immediately using an enrichment kit for ubiquitin (Thermo Scientific) according to the manufacturer's instructions. Levels of ubiquitin were analyzed by Western blot.

Flowcytometry. Unless otherwise stated, all analyses were performed by FACSCalibur flow cytometer (BD Biosciences) and at least 10,000 cells were analyzed for each condition. To detect loss of $\Delta\psi_m$ at 16 h cells were stained in 250 μ L RPMI containing 10 μ M 5,5',6,6-tetrachloro-1,1,3,3'-tetraethylbenzimidazolylcarbocyanine iodide (JC-1, Molecular probes) for 15 min, washed, scraped and analyzed. Loss of $\Delta\psi_m$ was demonstrated by a loss of fluorescence on the FL-2 channel as previously described (2). AM and lymphocyte surface marker expression was measured by incubating cells with 100 mg/ml human IgG1 (Sigma) to block Fc γ receptors then for at least 30 minutes at 4°C with fluorophore conjugated antibodies and appropriate isotype controls at concentrations of 0.1-0.25 μ g per 10⁵ cells in 100 μ L of 0.1% BSA in PBS (FACS buffer) according to the manufacturers' instructions as follows. AM were dually stained with

mouse anti-human CD206, (19.2), (APC), (eBioscience), and either mouse anti-human CD163, (GHI/61), (PE), (eBioscience), mouse anti-human CD80, (2D10.4), (PE), (eBioscience) or mouse anti-human CD200r, (OX108), (PE), (eBioscience). Gates were set on FSC/SSC to exclude debris and identify intact cells. APC (CD206⁺) geometric mean fluorescence intensity (MFI) expression was measured on this subpopulation using the FL4-H channel. PE (CD80⁺ / CD163⁺ / CD200r⁺) MFI for each conjugated antibody was measured on the CD206⁺ gated subpopulation using the FL2-H channel (Supplemental Figure 2B). Values were expressed as the ratio of the MFI of the marker (APC or PE) to the MFI of the isotype control. Lymphocytes were stained with mouse anti-human anti-CD3 (SK7) phycoerythrin (PE), (eBioscience), mouse anti-Human CD38 (HB7), fluorescein isothiocyanate (FITC), (eBioscience), mouse anti-human anti-CD4 (S3.5), allophycocyanin (APC), (Invitrogen) and mouse anti-human CD8, (RPA-T8), (Brilliant Violet 421), (Biolegend) for lymphocytes and LIVE/DEAD® Blue Fixable Dead Cell Stain Kit (L23105, Molecular Probes, Invitrogen). In parallel anti-mouse Ig kappa and negative control compensation beads (BD™ Compbeads, BD Biosciences) were incubated with each antibody conjugate separately. Labeled cells were then analyzed on a 13 color LSRII™ (BD Biosciences) flow cytometer. The beads were used to set a compensation matrix, unstained cells were used to set FSC and SSC, and isotype control labeled cells used to set the red 633nm (660/20 filter, APC), blue 488 nm (575/26 filter, PE and 530/30 filter FITC), violet 405nm (450/40 filter, brilliant violet), and UV 355nm (450/40 filter UV) laser voltages and filters. These were then kept the same for each subsequent donor sample. Lymphocytes were identified on FSC/SSC. Doublet cells were excluded using a FSC-A versus FSC-H event plot. Cells with high UV 450/40 (LIVE/DEAD® Blue) intensity on the singlet cell gate were considered to be dead lymphocytes and excluded. T lymphocytes were identified as CD3⁺ cells, defined as blue

575/26⁺ events in the live cell population. Back gating was performed to confirm that the CD3⁺ cells were within the original lymphocyte gate on FSC/SSC. CD4⁻/CD8⁺ (CD8⁺ T lymphocyte) cells were defined as violet 450/40⁺ red 660/20⁻ events and CD4⁺/CD8⁻ (CD4⁺ T lymphocyte) cells were defined as violet 450/40⁻ red 660/20⁺ within the CD3⁺ population (Supplemental Figure 2D). The expression of CD38 on CD8⁺ T cells was defined as the ratio of the MFI on the blue 530/30 channel for CD3⁺/CD4⁻/CD8⁺ gated events to that of isotype control. Data analyses were performed using FlowJo™ software version 9.3.2 (Tree Star, Inc.).

Measurement of Mitochondrial Reactive Oxygen Species (mROS). mROS production was measured at 16 h by incubating macrophages with 2.5 μM MitoSOX™ Red (Invitrogen) for 15 min at 37°C. This cell permeable dye contains dihydroethidine which targets mitochondria and undergoes O₂⁻-dependent hydroxylation to 2-hydroxyethidium which fluoresces at excitation/emission spectra of 400/590nm. Cells were washed with Hank's Balanced Salt Solution (HBSS, Gibco), and fluorescence measured on scraped cells by FACSCalibur using 488 nm excitation to measure oxidized MitoSOX™ Red in the FL2 channel. Because MitoSOX™ Red cannot be used on fixed cells HIV-1/sham infected MDM were analyzed directly using a Varioskan Flash multimode reader (Thermo Scientific) in containment level 3 conditions. To control for number of mitochondria, cellular mitochondrial mass was measured in matched wells using MitoTracker™ Green FM (Invitrogen).

Microscopy. Apoptosis detection. Nuclear morphology was examined by in 4', 6-diamidino-2-phenylindole (DAPI, Vectorshield™, Vector Laboratories) using a fluorescent light microscope (Leica, DMRB 1000) at 1000x magnification using a 100x/1.30 (PL Fluotar) objective at room temperature. Blinded reviewers counted 300

cells on duplicate coverslips mounted on glass slides for the presence of condensed or fragmented nuclei, to estimate apoptosis as previously described (2). MDM treated with 5 μ M staurosporine (Sigma-Aldrich) were used as a positive control. *BAL cell identification*. BAL cells were identified using light microscopy (Nikon, Eclipse TE300) of Diff-Quick stained (Dade Behring) cytopins at 1000x magnification using a 100x/1.25 oil emersion (Nikon Plan) objective. At least 300 cells were counted. *HIV-1_{BAL} MDM imaging*. MDM stained for p24 were imaged with a Leica DMRB microscope at 400x magnification using a 40x objective and imaging software (SPOT Advanced Imaging Software).

Caspase activation. Macrophage caspase 3/7 activity was measured directly in culture wells at 16 h using the Caspase-Glo™ 3/7 assay (Promega) in accordance with the manufacturer's instructions. Luminescence was measured on a Varioskan Flash multimode reader (Thermo Scientific).

Quantification of gp120 by ELISA. gp120 in BAL was quantified by ELISA. High Binding plates (Costar) were coated with 1mg/mL with each of three human monoclonal Abs against gp120: 14E, 17B, EH21 (kindly provided by James E Robinson, Tulane University, New Orleans). After blocking with 1% ovalbumin, BAL fluid supernatants were concentrated by approximately 12 fold using 50k Amicon Ultra filter (Merck Millipore) and added to the plate and gp120 detected using a 1/2000 dilution of the same biotinylated antibodies (6). Two-fold serial dilutions of recombinant gp120 (HIV-1_{LAI/IIIB}) were used as standards and results considered positive if above the limit of detection in the linear range of a log/lin standard curve, giving a lower limit of detection in the ELISA of 25ng/mL and BAL fluid of 2ng/mL. BAL fluid samples from 6

HIV-1-seronegative donors were used as negative controls or spiked with recombinant gp120 for positive controls.

Intracellular Bacterial Killing assay. Assessment of intracellular bacterial viability was carried out at 4 h and 20 h as previously described (7). Briefly, cells were infected and at 4 h washed x 3 in PBS then incubated for 30 minutes in fresh medium containing 40 units/mL benzyl penicillin (Crystapen™, Genus Pharmaceuticals) and 20 µg/mL gentamicin (Cidomycin™, Sanofi) to kill extracellular bacteria before being lysed with 2% saponin (Sigma) for 12 min. Lysates were diluted to 1ml in PBS, and intracellular bacterial numbers determined by Miles-Misra surface viable count. Alternatively following penicillin/gentamicin treatment cells were returned to the incubator in medium containing 0.7 µg/mL vancomycin (Sigma) to ensure extracellular bacteria remained undetectable with an antimicrobial that lacked significant intracellular penetration then washed and lysed at 20 h and viable counts performed as before.

Real-time measurement of cell respiration. Macrophage mediated real-time mitochondrial respiration (e.g. OXPHOS) was measured by the XF24 extracellular flux analyzer (Seahorse, Bioscience). Briefly, 14 day MDM were detached from T27 culture flasks using accutase (Biolegend) and gentle scraping and re-seeded at 2x10⁵ well in an XF24 cell plate (Seahorse Bioscience) and left to re-adhere. Following pneumococcal challenge in the presence or absence of gp120 wells were washed with XF medium (Seahorse, Bioscience) that had been supplemented with 4.5g/L D-glucose, 2mM L-glutamine, 1.0mM Na-pyruvate and penicillin (100U/mL and streptomycin (100µg/mL) and adjusted to pH 7.4 with 1.0M NaOH and then incubated for an hour at 37°C without CO₂ in 630µL/well of the same XF medium with or without gp120. The XF24 utility plate was submerged in XF calibrant (Bioscience) and incubated for 16 h at 37°C. The ATP

synthase inhibitor oligomycin A (70 μ L at 15 μ M), the mitochondrial uncoupler FCCP (77 μ L at 20 μ M) and the combination of the complex I inhibitor rotenone and complex III inhibitor antimycin A (85 μ L at 10 μ M) were added to the cartridge containing injection ports A, B and C respectively and incubated for an hour at 37°C without CO₂ supplementation. An XF24 analyser was then used to measure the rate of oxygen consumption (OCR) and extracellular acidification (ECAR) kinetically before and after injecting oligomycin (1.5 μ M, the final concentration), FCCP (2.0 μ M) and rotenone (1.0 μ M) plus antimycin A (1.0 μ M) (Sigma Aldrich) as per the manufacturer's instructions. Cells were then lysed with mammalian cell lysis buffer (ThermoFisher) plus protease inhibitors cocktail (Roche) and the total protein was estimated by the Bradford method and kits (Bio-Rad). Baseline ECAR, basal OCR, ATP linked OCR, maximum respiration capacity and mitochondrial inner membrane mediated proton leak were calculated from ECAR and OCR measurement after normalization for protein content using the formula described by Zhang J et al. (8).

RT-PCR Array. After 48 h in culture AM were washed 3 times to remove non-adherent cells, a technique which has been demonstrated to yield a purity of 98% viable AM (4), then harvested in Tri Reagent (Sigma) and preserved at -80°C. Total RNA was extracted using a Direct Zol RNA miniprep kit (Zymo research). Nucleic acid concentration was measured using a Nanodrop spectrophotometer (ThermoFisher Scientific) and RNA quality (RNA integrity number) was assessed with an Agilent BioAnalyzer following the Nano Kit Lab-On-A-Chip procedure (Agilent Technologies). The cDNA template was synthesized from RNA with a RIN > 7.5 with a RT² First Strand Kit (SABiosciences) and cDNA product visualized by Agarose Gel Electrophoresis following PCR amplification with a housekeeping gene (β actin) primer. cDNA was analyzed for expression of genes

associated with apoptosis and macrophage activation and 11 housekeeping genes (Supplemental Figure I) with a custom made primer/probe sets on a RT² Profiler PCR Array (SABiosciences) using the Mx3000P QPCR System (Agilent). Ct values were gathered and data analysis was performed via the $\Delta\Delta\text{Ct}$ method using PCRArrayDataanalysis_V4 software (SABiosciences) to determine relative expression differences between the comparison groups with reference to the housekeeping genes. Changes of mRNA abundances by 2-fold and higher with a p value <0.05 calculated based on a Student's t-test of the replicate $2^{(-\Delta\text{Ct})}$ values for each gene in the control group and treatment groups, and a q value calculated by correcting for multiple testing using the method of Benjamini and Hochberg (1) with a false discovery rate of 1%, were considered significantly different between the comparison groups.

Ultra-sensitive detection of HIV-1 RNA in BAL. BAL HIV-1 RNA was quantified using a modified version of the Abbott Real Time HIV-1 assay (Maidenhead, UK), following ultracentrifugation of up to 12 ml of BAL at 240,000 g for 20min at 4°C, and resuspension of the pellet in 1 ml of the supernatant, similarly to what has been recently applied in plasma samples (9). Modified assay sensitivity was determined by spiking 12 ml of acellular BAL obtained from HIV-negative volunteers with the World Health Organization (WHO) 3rd International HIV-1 RNA Standard (NIBSC code:10/152, Hertfordshire, UK) at concentrations of 1 and 8 copies/ml in triplicate. The sensitive protocol showed a lower limit of detection (LLD) 1 copy/ml, which ranged from 1-2 copies per mL (cps/mL) depending on the initial input volume of BAL. Inhibition in BAL samples was also tested using acellular BAL supernatants and plasma obtained from HIV-seronegative volunteers spiked in parallel with four dilutions (100, 500, 1000, 5000

and 10000 copies/ml) of the WHO 3rd International HIV-1 RNA Standard and tested in duplicate. No inhibition occurred when testing BAL samples. *Sample measurement:* Up to 12mL (median 12ml; IQR: 10.25, 12.00) of each BAL sample was ultracentrifuged and HIV-1 RNA was quantified using the sensitive protocol. 7 of 13 (54%) samples had sufficient volume to allow testing in duplicate.

Statistics

Results are recorded as mean and SEM unless otherwise stated. Sample sizes were informed by standard errors obtained from similar assays in prior publications (2, 10). Decisions on use of parametric or non-parametric tests were based upon results of D'Agostino-Pearson normality tests. Parametric or nonparametric testing was performed with the indicated tests using Prism 6.0 software (GraphPad Inc.). Comparisons between two conditions were performed using a paired or unpaired t-test for parametric data, or a Mann-Whitney U test or Wilcoxon signed rank test for non-parametric data. Correlation was measured with two-tailed Pearson. When two or more conditions were assessed in two experimental groups (e.g. HIV-1-seropositive vs. HIV-seronegative), data were analyzed by ANOVA with Holm-Sidak post-tests. Significance was defined as $p < 0.05$.

Supplemental References

1. Benjamini Y, Hochberg Y. Controlling the False Discovery Rate - a Practical and Powerful Approach to Multiple Testing. *J Roy Stat Soc B Met* 1995; 57: 289-300.
2. Marriott HM, Bingle CD, Read RC, Braley KE, Kroemer G, Hellewell PG, Craig RW, Whyte MK, Dockrell DH. Dynamic changes in Mcl-1 expression regulate macrophage viability or commitment to apoptosis during bacterial clearance. *J Clin Invest* 2005; 115: 359-368.
3. Tsang J, Chain BM, Miller RF, Webb BL, Barclay W, Towers GJ, Katz DR, Noursadeghi M. HIV-1 infection of macrophages is dependent on evasion of innate immune cellular activation. *AIDS* 2009; 23: 2255-2263.
4. Gordon SB, Molyneux ME, Boeree MJ, Kanyanda S, Chaponda M, Squire SB, Read RC. Opsonic phagocytosis of *Streptococcus pneumoniae* by alveolar macrophages is not impaired in human immunodeficiency virus-infected Malawian adults. *J Infect Dis* 2001; 184: 1345-1349.
5. Bewley MA, Marriott HM, Tulone C, Francis SE, Mitchell TJ, Read RC, Chain B, Kroemer G, Whyte MK, Dockrell DH. A cardinal role for cathepsin d in coordinating the host-mediated apoptosis of macrophages and killing of pneumococci. *PLoS Pathog* 2011; 7: e1001262.
6. Rychert J, Strick D, Bazner S, Robinson J, Rosenberg E. Detection of HIV gp120 in plasma during early HIV infection is associated with increased proinflammatory and immunoregulatory cytokines. *AIDS Res Hum Retroviruses* 2010; 26: 1139-1145.
7. Marriott HM, Ali F, Read RC, Mitchell TJ, Whyte MK, Dockrell DH. Nitric oxide levels regulate macrophage commitment to apoptosis or necrosis during pneumococcal infection. *FASEB J* 2004; 18: 1126-1128.

8. Zhang J, Nuebel E, Wisidagama DR, Setoguchi K, Hong JS, Van Horn CM, Imam SS, Vergnes L, Malone CS, Koehler CM, Teitell MA. Measuring energy metabolism in cultured cells, including human pluripotent stem cells and differentiated cells. *Nat Protoc* 2012; 7: 1068-1085.

9. Ruggiero A, De Spiegelaere W, Cozzi-Lepri A, Kiselinova M, Pollakis G, Beloukas A, Vandekerckhove L, Strain M, Richman D, Phillips A, Geretti AM, Group ES. During Stably Suppressive Antiretroviral Therapy Integrated HIV-1 DNA Load in Peripheral Blood is Associated with the Frequency of CD8 Cells Expressing HLA-DR/DP/DQ. *EBioMedicine* 2015; 2: 1153-1159.

10. Bewley MA, Preston JA, Mohasin M, Marriott HM, Budd RC, Swales J, Collini P, Greaves DR, Craig RW, Brightling CE, Donnelly LE, Barnes PJ, Singh D, Shapiro SD, Whyte MKB, Dockrell DH. Impaired Mitochondrial Microbicidal Responses in Chronic Obstructive Pulmonary Disease Macrophages. *Am J Respir Crit Care Med* 2017.

Supplemental Figure Legends

Figure E1 The expression of genes associated with macrophage activation and apoptosis regulation is not altered in alveolar macrophages in people living with HIV.

Expression levels of genes regulating macrophage activation and apoptosis in overnight rested alveolar macrophages (AM) from control (n=5) and ART treated HIV-1⁺ (n=8) donors, measured by customized RT²Profiler PCR array (Qiagen) and normalized to 11 housekeeping genes (A). The mean Log₂ fold difference in CT value ($\Delta\Delta CT$) between HIV-1 and control donors is plotted against Log p value (B). Entrez Gene Official Symbols for housekeeping genes and genes of interest (GOI) are listed with the fold change in expression (FC) in AM from ART treated HIV-1⁺. p values are calculated based on a Student's t-test of the replicate $2^{(-\Delta Ct)}$ values for each gene in the control group and treatment groups and q values calculated with a false discovery rate of 1% (C).

Figure E2 Flow cytometry gating strategy illustrating no alteration in alveolar macrophage surface markers associated with polarization but altered pulmonary CD4⁺:CD8⁺ T cell ratio in HIV.

Bronchoalveolar lavage (BAL) cells from control (n=6) and ART treated HIV-1⁺ (ART, n=11) donors were enriched for alveolar macrophages (AM) by overnight plastic adhesion. AM were identified as CD206⁺ and surface expression of CD80 (M1), CD206, CD163 and CD200r (M2) compared between groups by flow cytometry (A). Representative histograms for each surface marker conjugate

(shaded) and isotype control (empty) are shown for a healthy donor (control) and ART treated HIV-1+ donor (B). AM were identified on forward scatter (FSC) and side scatter (SCC), laser voltages were set such that APC/PE isotype controls were in the first log, CD206 expression measured on the FL4 channel and CD80, CD163 or CD200r expression measured on FL2 and the MFI of each antibody conjugate and its isotype control were compared to derive the geometric mean ratio (GMR) (C). 24 h after BAL, non-adherent cells were washed and labeled with anti-CD3-PE, anti-CD4-APC, anti-CD8-brilliant violet, and a viability dye. Upper panel: Lymphocytes were identified by forward (FSC) and side scatter (SSC) and doublets excluded using FSC-area (FSC-A) /FSC-height (FSC-H). Events expressing $>1 \log_{10}$ higher than unstained on UV 450/40 (UV live dead) were considered dead and excluded. Viable cells with high blue 575/26 (PE) expression were gated as CD3⁺. CD3⁺ cells expressing high red 660/20 (APC) and low violet 450/50 (brilliant violet) were classified as CD4⁺ T cells and those with low red 660/20 and high violet 450/50 were classified as CD8⁺ T cells. Cells incubated with PE, APC and brilliant violet conjugated isotype control antibodies are shown for comparison in the lower panel. Events numbers on each gate are percentages of parent gate. Representative plots from an ART donor are shown with those from a control donor on the right hand end (D). Box plots show median, IQR and range. MFI= geometric mean fluorescence intensity, IC=isotype control, APC = allophycocyanin, PE = phycoerythrin.

Supplemental Figure E3 Co-Culture with CD8⁺ T-cells does not modulate macrophage apoptosis or intracellular bacterial killing

Monocyte-derived macrophages (MDM) were co-cultured on their own or with autologous CD8⁺ lymphocytes that were either treated with control beads or activated with Dynabeads Human T-Activator CD3/CD28 for 2 h. MDM were then mock-infected (MI) or challenged with *Streptococcus pneumoniae* (D39) and the number of viable MDM (A), the percentage of fragmented or condensed nuclei (B) or intracellular bacterial survival at 4 h and 20 h estimated (C) n=4. ns = no significant interaction for CD8 co-culture, 2 way ANOVA.

Figure E1 A

Housekeeping genes

HMBS
RPS16
GAPDH
ACTB
PPIA
B2M
HPRT1
RPLP0
GUSB
RPLP1
TBP

Figure E1 B

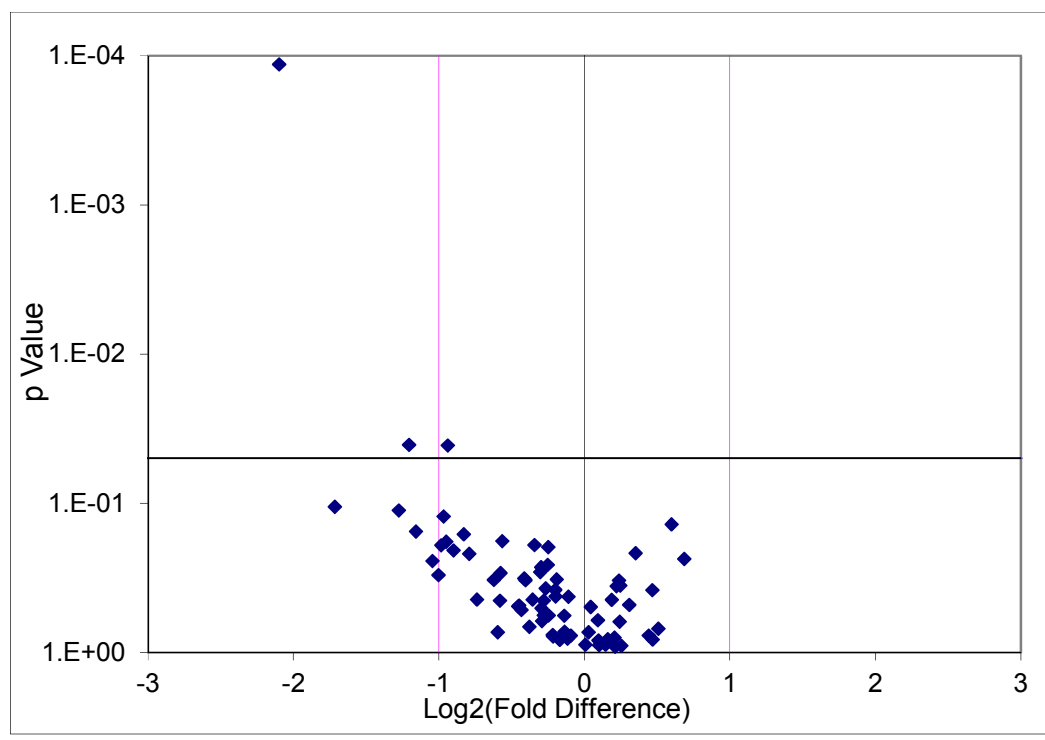
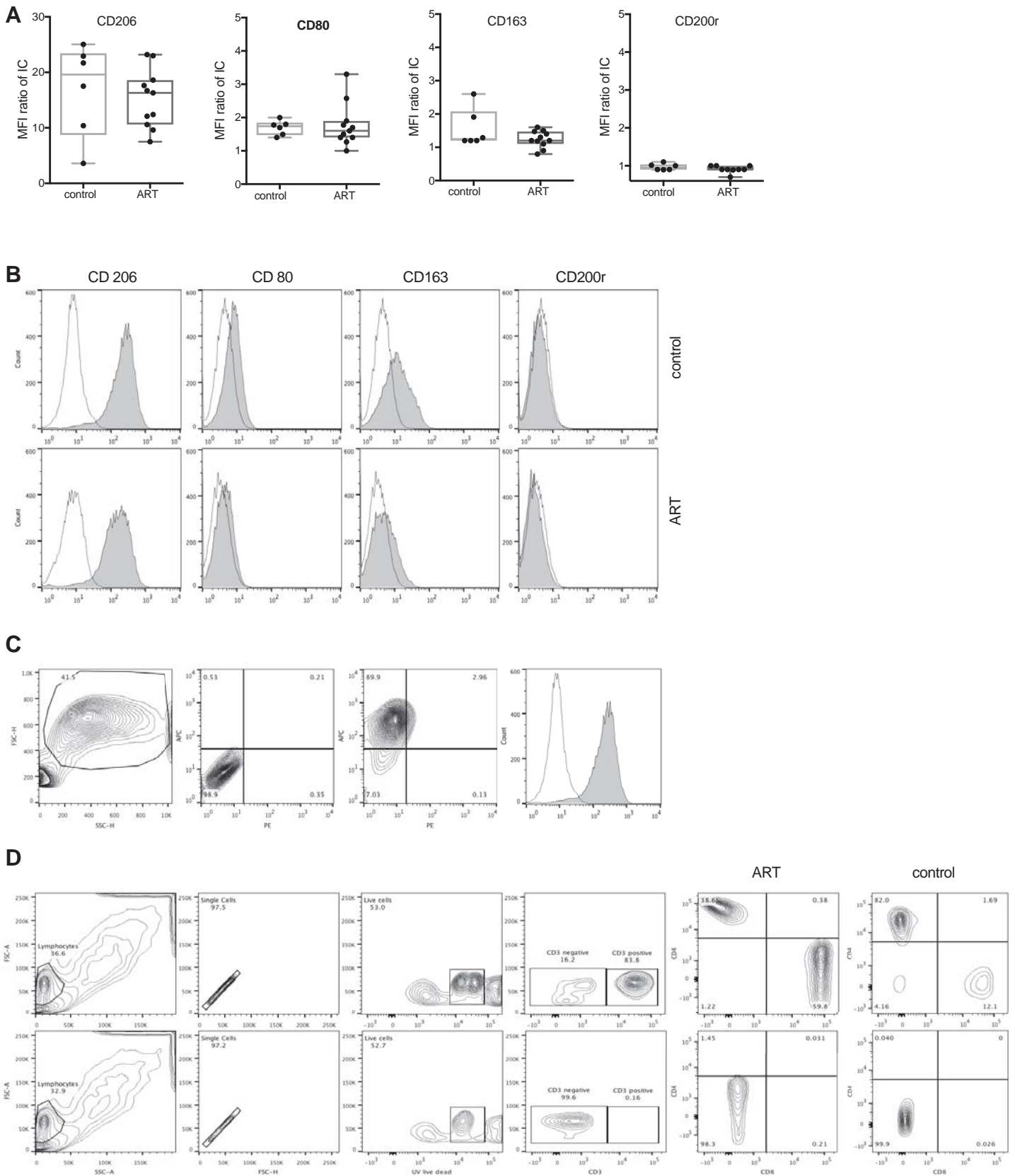


Figure E1 C

GOI	FC	p value	q value	GOI	FC	p value	q value
HUWE1	-0.28	0.5659	0.8380	AKT3	-0.17	0.8210	0.8925
EEF2K	-0.38	0.6728	0.8925	PTEN	-0.34	0.1908	0.8111
TNFSF10	0.21	0.7973	0.8925	GSK3B	-0.14	0.5662	0.8380
FASLG	-0.29	0.6158	0.8711	IL15	0.60	0.1382	0.8111
TNFRSF10A	-0.43	0.5189	0.8170	IL1B	-1.05	0.2440	0.8111
TNFRSF10B	-0.30	0.5056	0.8134	CCL22	-0.74	0.4409	0.8111
TNFRSF10C	0.47	0.8173	0.8925	CCL3	-0.83	0.1612	0.8111
TNFRSF10D	-0.22	0.7651	0.8925	CCL4	-0.95	0.1813	0.8111
SPATA2	-0.62	0.3269	0.8111	CXCL10	0.44	0.7700	0.8925
TNF	0.47	0.3832	0.8111	IL10	-0.97	0.1225	0.8111
CD209	-0.94	0.0410	0.8111	CCL15	0.51	0.6940	0.8925
IL12B	-0.25	0.1971	0.8111	CCL2	-2.10	0.0001	0.0084
NFE2L2	-0.19	0.3231	0.8111	CXCL3	-1.00	0.3025	0.8111
MAP3K5	-0.25	0.5640	0.8380	IL1A	-1.28	0.1117	0.8111
CFLAR	-0.14	0.7259	0.8925	IL6	-1.16	0.1548	0.8111
CX3CL1	-0.40	0.3283	0.8111	IL8	-0.36	0.4420	0.8111
BCL2L1	-0.30	0.2891	0.8111	MMP12	-0.98	0.1914	0.8111
BCL2	-0.56	0.1792	0.8111	PTGS2	0.09	0.6070	0.8711
BAX	-0.20	0.4219	0.8111	RIPK2	0.24	0.6239	0.8711
BAD	-0.25	0.2586	0.8111	CCL5	-0.58	0.2935	0.8111
MCL1	0.24	0.3300	0.8111	CD80	0.10	0.8322	0.8925
BID	0.35	0.2162	0.8111	CD86	0.14	0.8856	0.9138
BCL2A1	0.19	0.4446	0.8111	CXCL11	0.25	0.9014	0.9138
TP53	-0.45	0.4850	0.8134	CXCL9	-0.79	0.2180	0.8111
BBC3	-0.14	0.7603	0.8925	GBP5	0.21	0.9161	0.9161
PMAIP1	0.03	0.7314	0.8925	TNFSF10	0.16	0.8150	0.8925
APAF1	-0.58	0.4490	0.8111	CCR5	-0.60	0.7328	0.8925
PERP	-0.11	0.4243	0.8111	CD36	0.69	0.2358	0.8111
IER3	-1.72	0.1054	0.8111	MMP2	-1.21	0.0405	0.8111
USP9X	-0.20	0.3800	0.8111	MMP7	-0.90	0.2073	0.8111
EEF2	-0.30	0.2687	0.8111	SOD1	0.24	0.3573	0.8111
FAS	0.01	0.8849	0.9138	SOD2	-0.42	0.3195	0.8111
BCL2L11	-0.46	0.4904	0.8134	GSR	-0.09	0.7709	0.8925
FADD	0.10	0.8947	0.9138	TXN	0.31	0.4794	0.8134
PAK2	-0.28	0.4494	0.8111	HMOX1	0.04	0.4948	0.8134
AKT1	-0.27	0.3726	0.8111	NQO1	0.22	0.3599	0.8111
AKT2	-0.22	0.7812	0.8925	GPX2	-0.12	0.8083	0.8925



Supplemental Figure E2

